Avatars and Twins: Measurement-Data Driven Field Simulations

Stephan Russenschuck, 07.09.2021
PhD School “I. Gorini” 2021

The Avatar and Twin (classical black-box measurement)

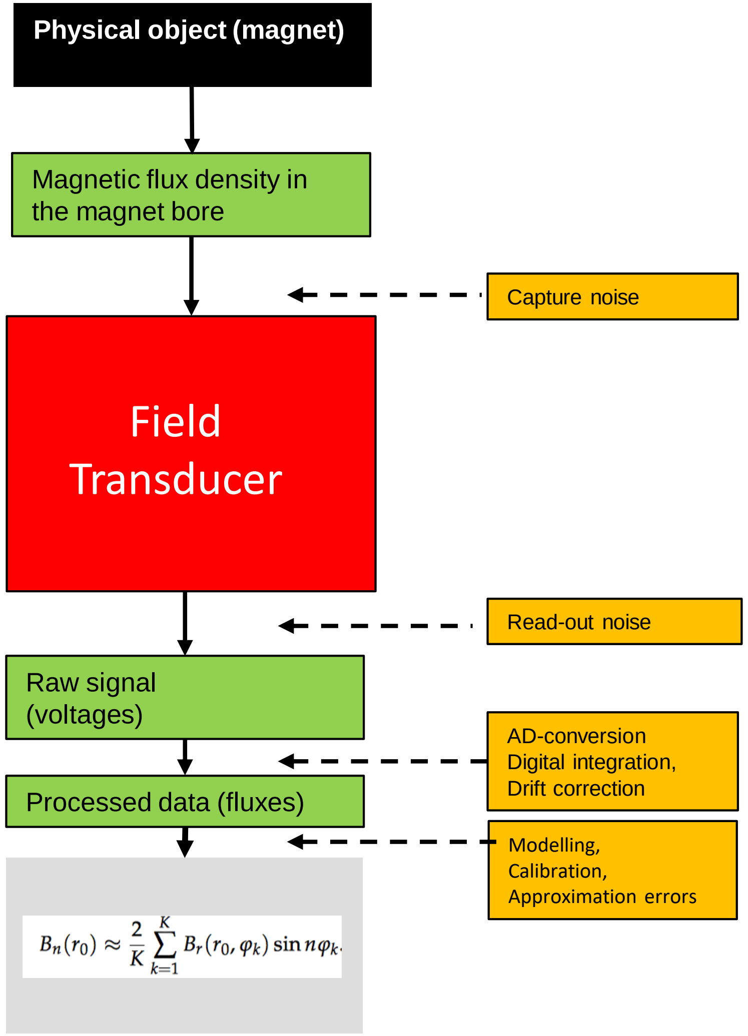

The Avatar and Twin (tracing of manufacturing tolerances and errors)

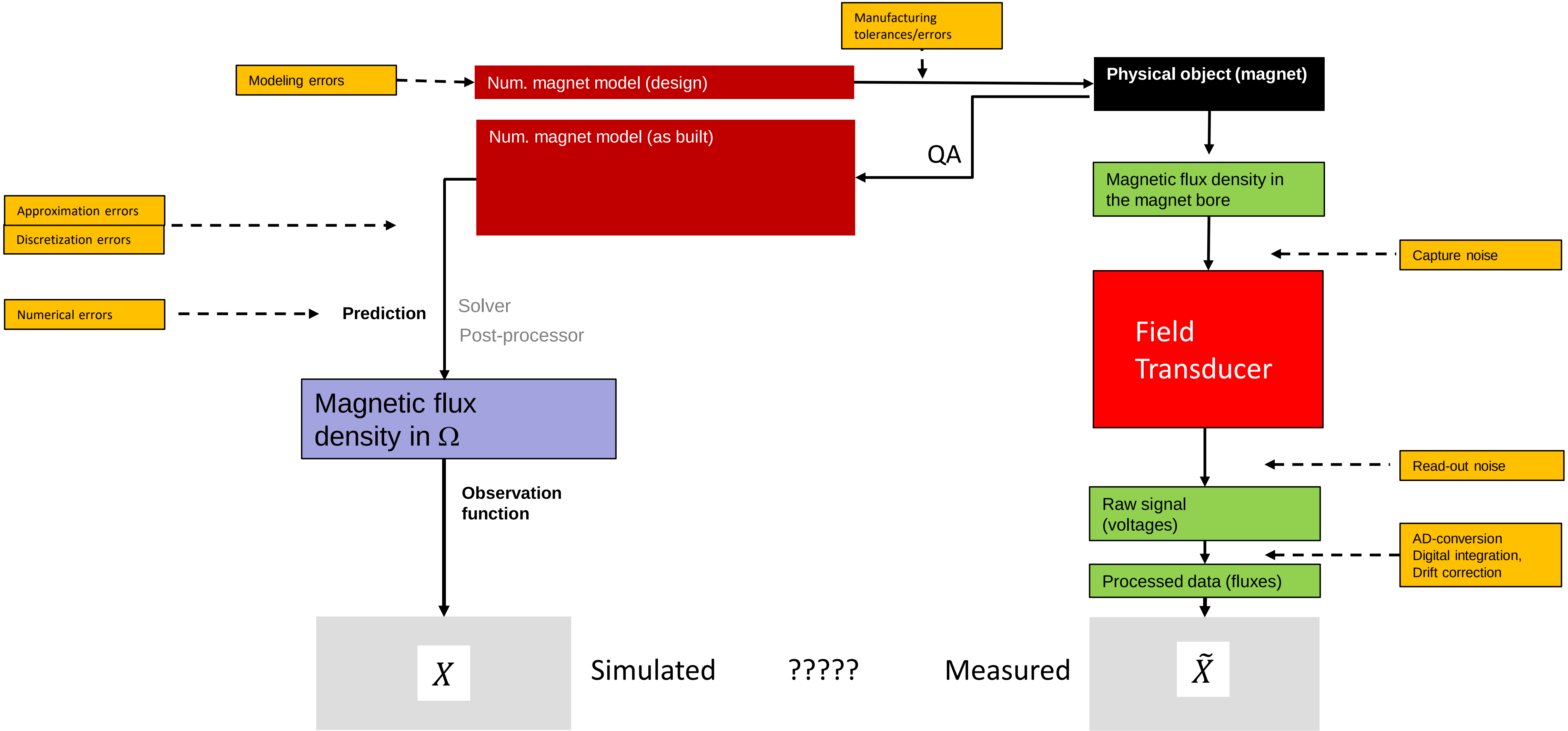

Beam Physicists, Magnet Designers, and Measurement Engineers

Everybody believes in measurements, but the measurement engineer himself.

Nobody believes in field simulations, but the field computation expert himself.

Establish “C3” coherence between magnetic measurements and needs for magnet design and production, and machine operation

Magnet Types

Coil Dominated Magnets

Normal Conducting (Bitter)

Superconducting

Class 1 (Detectors)

Class 2 (Accelerator)

Iron Dominated Magnets

Normal Conducting

Superferric

Permanent Magnet

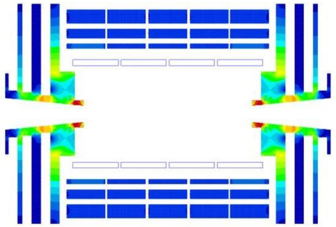

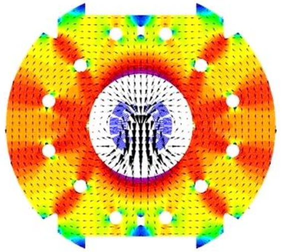

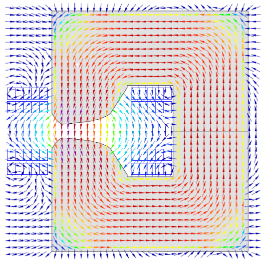

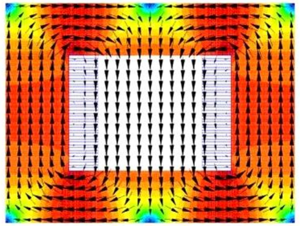

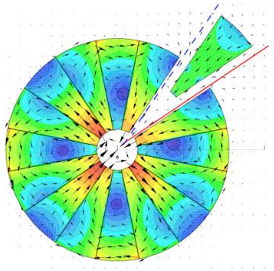

Iron Dominated Magnets

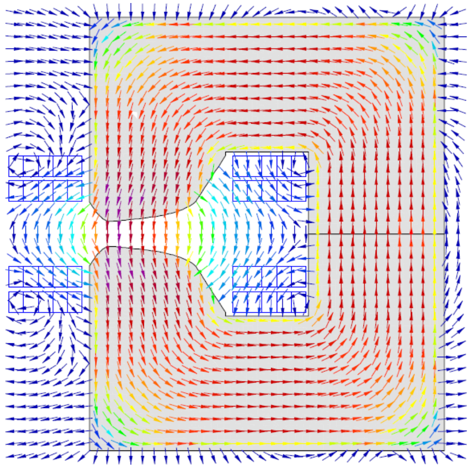

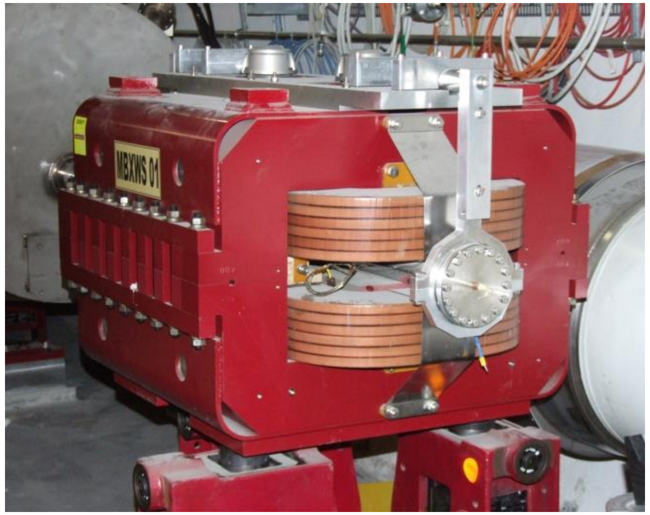

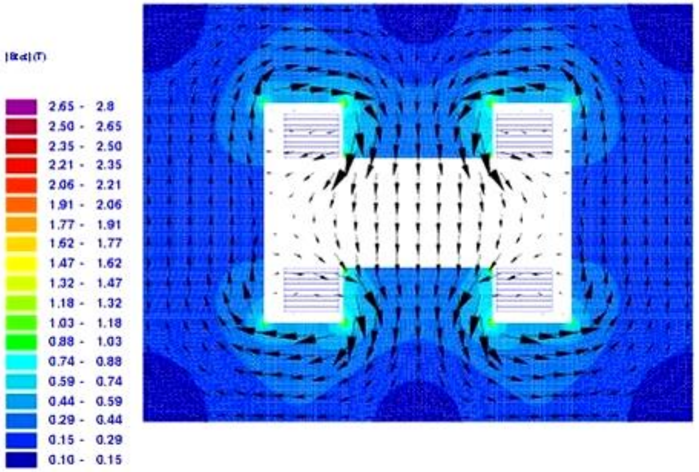

$N \cdot I = 24000$ A $\quad B_1 = 0.3$ T $\quad B_s = 0.065$ T $\quad$ Fill.fac. 0.98

Coil Dominated Magnets

Class 2

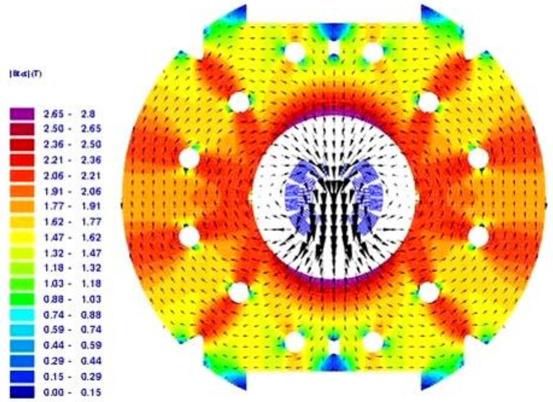

$B = 8.33$ T $B_s = 7.77$ T

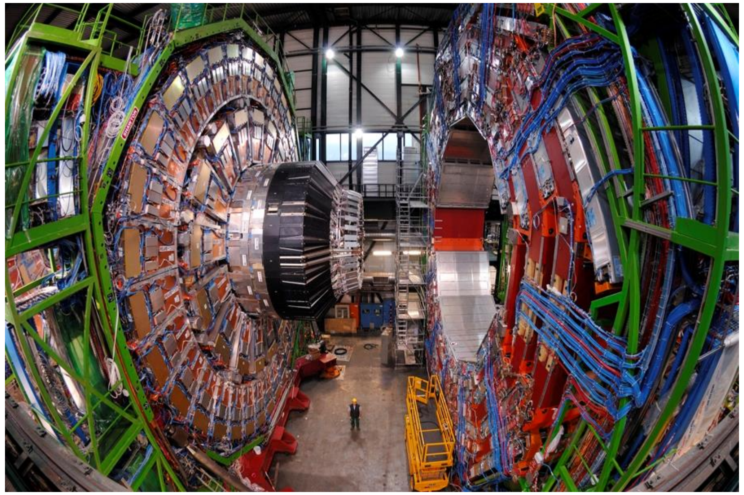

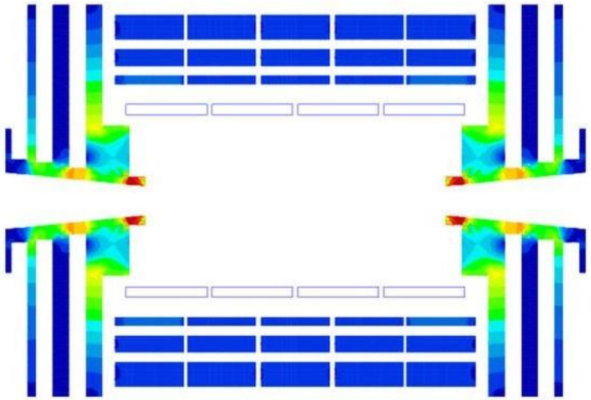

$B = 4$ T $B_s = 3.69$ T

Class 1

CMS (Class 1 Magnets)

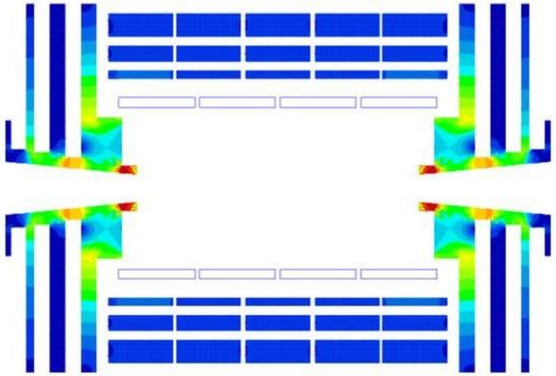

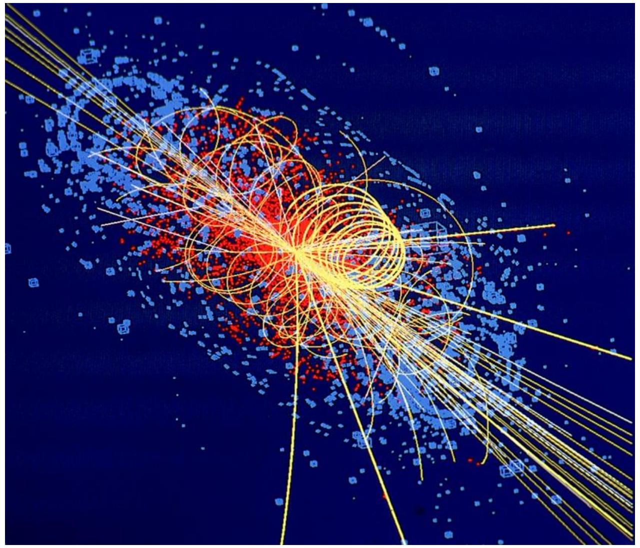

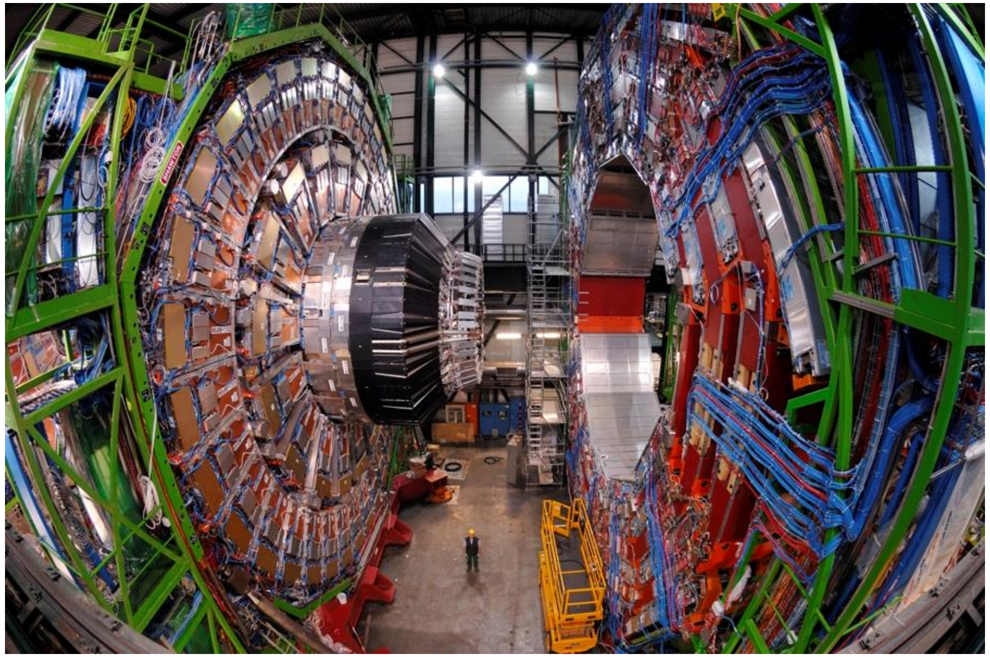

$$S = R(1 - \cos\frac{\alpha}{2}) \approx \frac{R\alpha^2}{8} = \frac{QBL^2}{8p}$$

- Normal conducting magnets
  - Important ohmic losses require water cooling
  - Field is defined by the iron pole shape (max 1.5 T)
  - Easy electrical and beam-vacuum interconnections
  - Voltage drop over one coil of the LHC-MBW magnets = 22 V

- Superconducting magnets
  - Field is defined by the coil layout
  - Maximum field limited to 10 T (NbTi), 14 T (Nb_3Sn)
  - Enormous electromagnetic forces (400 tons/m in MB for LHC)
  - Quench detection and magnet protection system required
  - Cryogenic installation (1.8 K)
  - Electrical interconnections in cryo-lines
  - Voltage drop on LHC magnet string (154 MB) 155 V

Renderings of the Same Vector Field

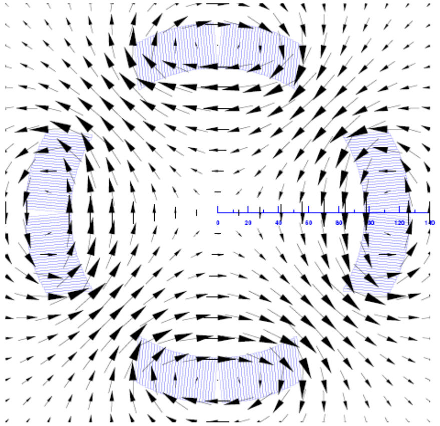

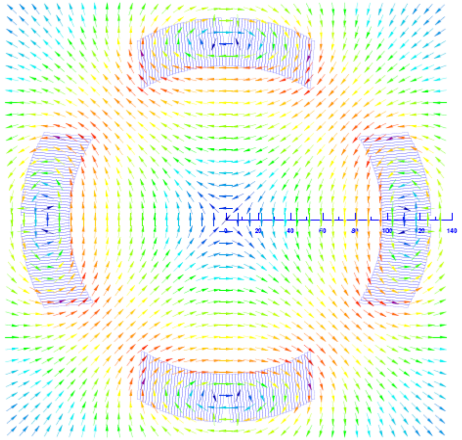

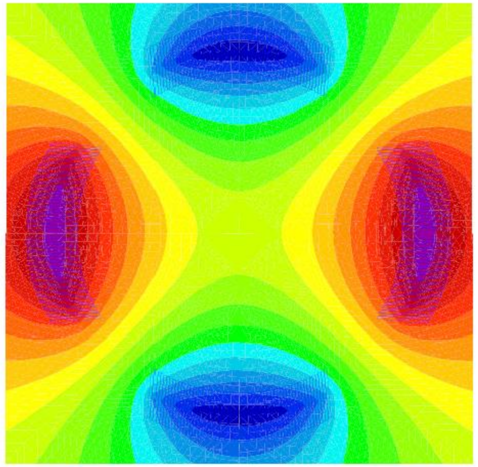

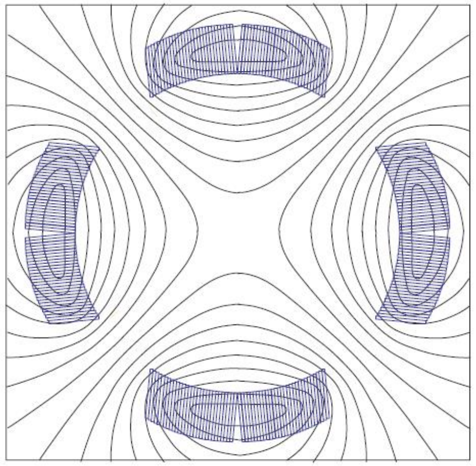

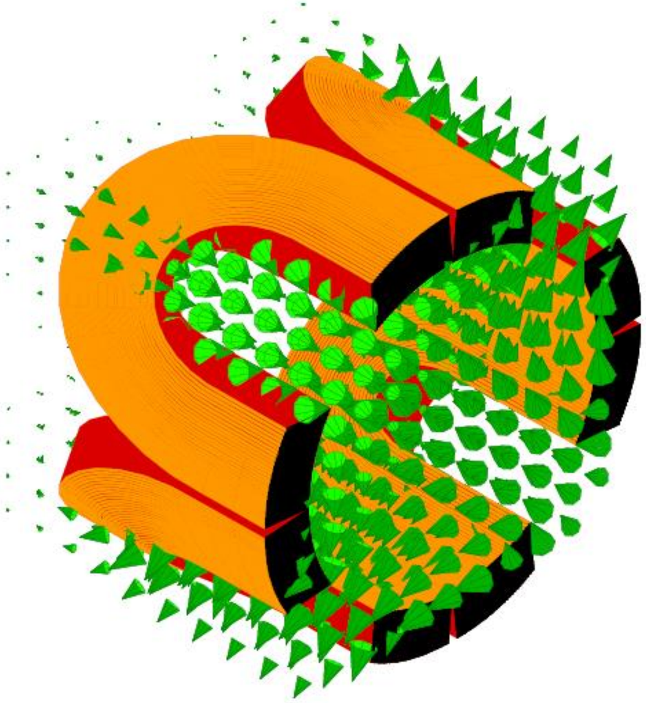

Maxwell’s Equations and the Regularity Conditions of Magnetic Fields

The simple form of constitutive equations are only true for linear (field-indep.), homogeneous (position-independ), isotropic (direction-indep.), lossless, and stationary media

Maxwell Equations

Integral Form

Local Form

Laplace’s Equation

Curl-Curl equation

Harmonic Fields

Green’s Functions

Weak-Forms

Kirchhoff

1D Calculation of normal conducting magnets

Field quality in accelerator magnets

The field of line-currents, coil-dominated magnets

FEM

BEM

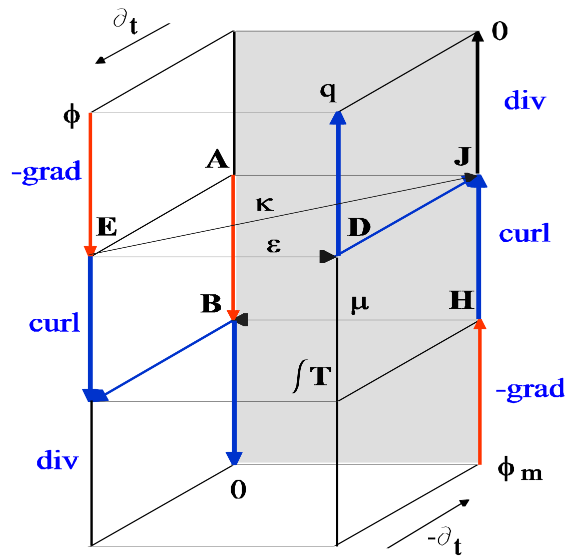

Required: Orientable manifolds, orientation, frame, metric, continuity, contractible domains

No switches, no Moebius strips, no internal boundaries, no holes in surfaces, no bubbles in volumes

$$\operatorname{curl}\frac{1}{\mu}\operatorname{curl}\mathbf{A} = \mathbf{J}$$

$$\frac{1}{\mu_0}\operatorname{curl}\operatorname{curl}\mathbf{A} = \mathbf{J}$$

$$\nabla^2\mathbf{A} - \operatorname{grad}\operatorname{div}\mathbf{A} = 0$$

$$\nabla^2 A_z = 0$$

Coulomb gauge !

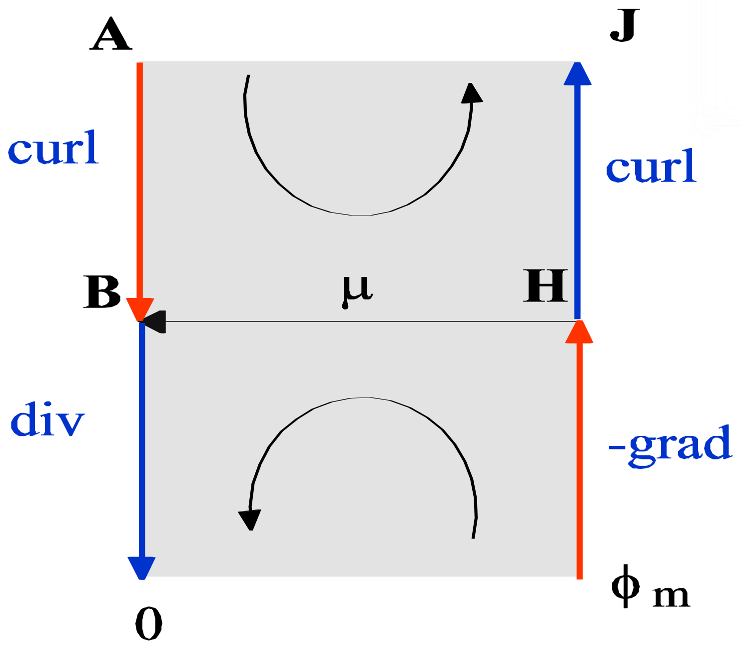

$$\operatorname{div}\mu\operatorname{grad}\phi_{\mathrm{m}} = 0$$

$$\mu_0\operatorname{div}\operatorname{grad}\phi_{\mathrm{m}} = 0$$

$$\nabla^2\phi_{\mathrm{m}} = 0$$

Field Quality

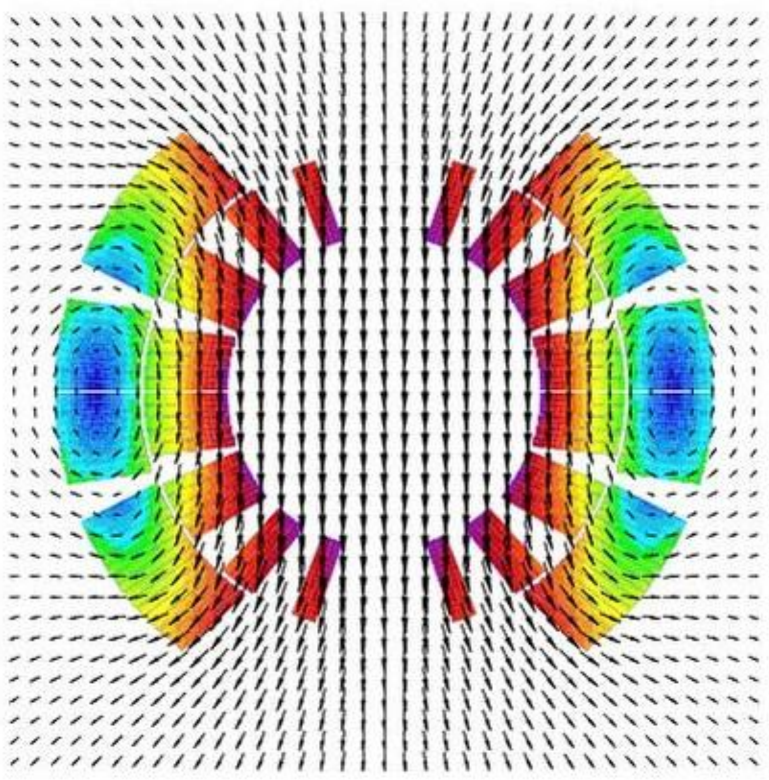

Field map

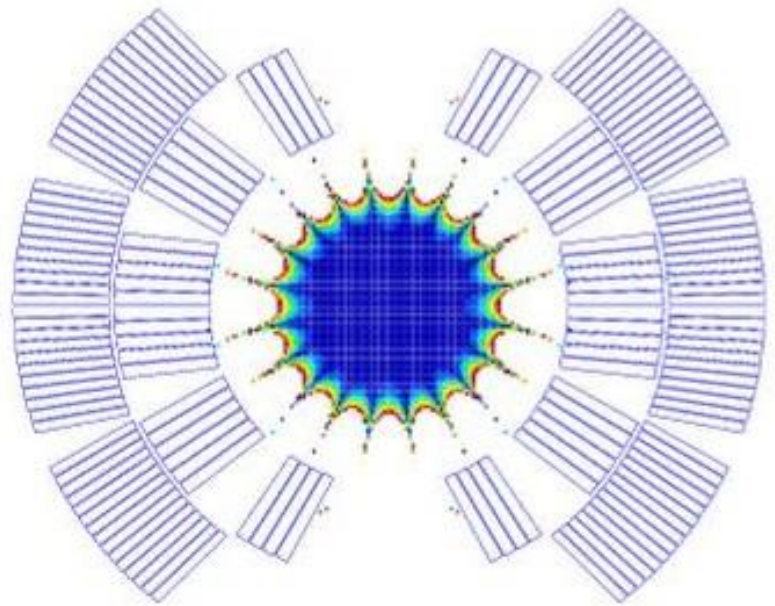

Good field region

Solving the Boundary Value Problem (1)

1. Governing equation in the air domain $\nabla^2 A_z = 0,$

2. Chose a suitable coordinate system

$$r^2 \frac{\partial^2 A_z}{\partial r^2} + r \frac{\partial A_z}{\partial r} + \frac{\partial^2 A_z}{\partial \varphi^2} = 0,$$

3. Find eigenfunctions. Coefficients are not known

$$A_z(r,\varphi) = \sum_{n=1}^{\infty} r^n (\mathcal{A}_n \sin n\varphi + \mathcal{B}_n \cos n\varphi).$$

4. Calculate a field component

$$B_r(r,\varphi) = \frac{1}{r}\frac{\partial A_z}{\partial \varphi} = \sum_{n=1}^{\infty} n r^{n-1} (\mathcal{A}_n \cos n\varphi - \mathcal{B}_n \sin n\varphi),$$

5. Measure (or calculate) the field on a reference radius and perform Fourier analysis (develop into the eigenfunctions). Coefficients are known

$$B_r(r_0,\varphi) = \sum_{n=1}^{\infty} (B_n(r_0) \sin n\varphi + A_n(r_0) \cos n\varphi),$$

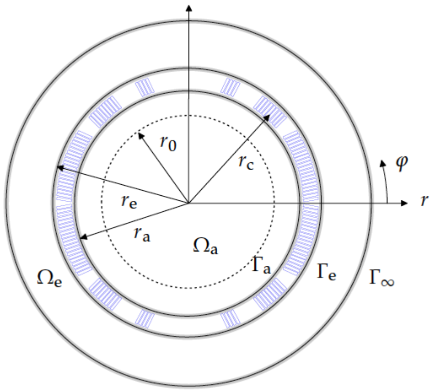

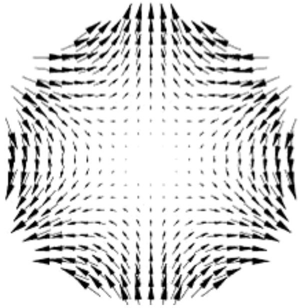

6. Compare the known and unknown coefficients

$$\mathcal{A}_n = \frac{1}{n\, r_0^{n-1}} A_n(r_0)\,, \qquad \mathcal{B}_n = \frac{-1}{n\, r_0^{n-1}} B_n(r_0)\,.$$

7. Put this into the original solution for the entire air domain

$$A_z(r,\varphi) = -\sum_{n=1}^{\infty} \frac{r_0}{n} \left(\frac{r}{r_0}\right)^n (B_n(r_0)\cos n\varphi - A_n(r_0)\sin n\varphi).$$

Take any 2π periodic function and develop according to

$$\frac{C_0}{2} + \sum_{n=1}^{\infty} (C_n(r_0)\sin n\varphi + D_n(r_0)\cos n\varphi)\,.$$

	B_r	B_φ	B_x	B_y	A_z	ϕ_{m}
$B_n =$	C_n	D_n	C_{n-1}	D_{n-1}	$\frac{-nD_n}{r_0}$	$\frac{-n\mu_0 C_n}{r_0}$
$A_n =$	D_n	$-C_n$	D_{n-1}	$-C_{n-1}$	$\frac{nC_n}{r_0}$	$\frac{-n\mu_0 D_n}{r_0}$

We can use fields, potentials, fluxes, or wire-oscillation amplitudes as “raw data”. The differential operators grad and rot transform into simple algebra in the L2 space of Fourier coefficients.

Objectives for the ROXIE Development

- ➔ Automatic generation of coil and yoke geometries
  - – Features: Layers, coil-blocks, conductors, strands, holes, keys
- ➔ Field computation specially suited for magnet design (Ar, BEM-FEM)
  - – No meshing of the coil
  - – No artificial boundary conditions
  - – Higher order quadrilateral meshes,
  - – Parametric mesh generator
  - – Modeling of SC magnetization
- ➔ Mathematical optimization techniques
  - – Genetic optimization,
  - – Pareto optimization,
  - – Search algorithms
- ➔ CAD/CAM interfaces

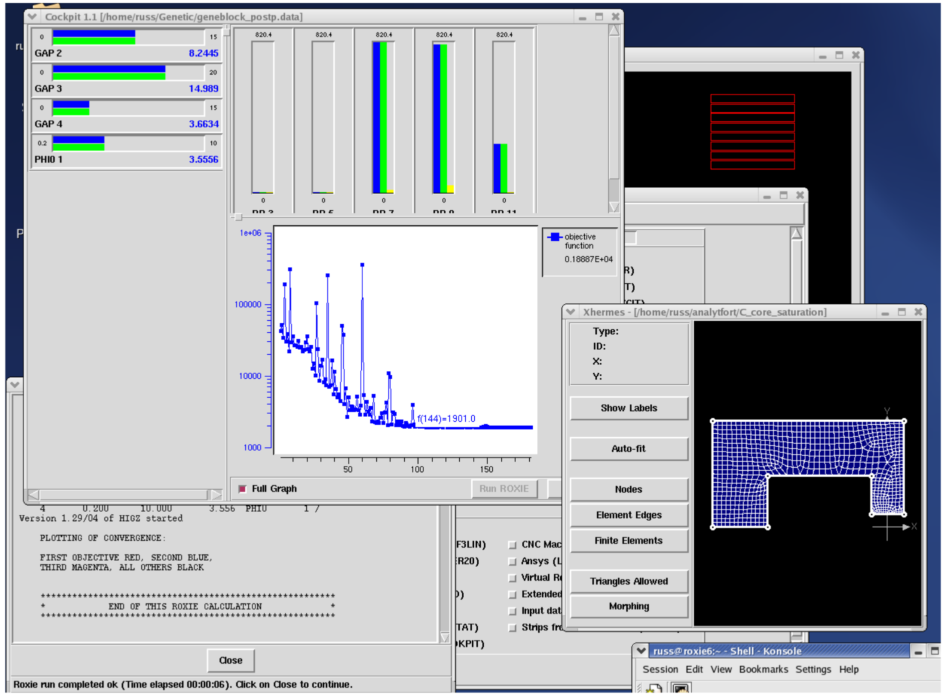

BEM-FEM Coupling

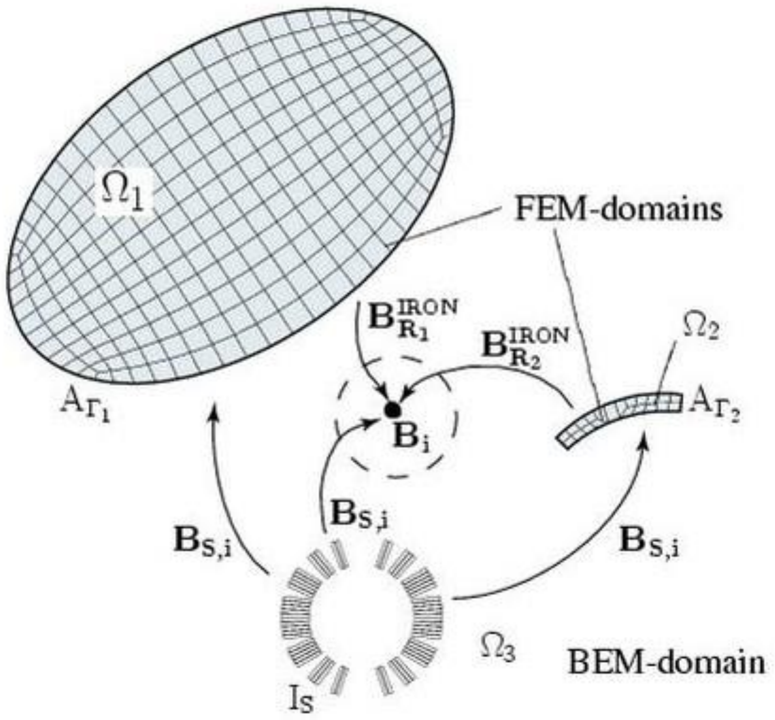

BEM

$$\{Q\} = -[G]^{-1}[H]\{A\} + [G]^{-1}\{A_s\}$$

FEM

$$[K]\{A\} - [T]\{Q\} = \{F(\mathbf{M})\}$$

$$\left([K] + [T][G]^{-1}[H]\right)\{A\} = \{F(\mathbf{M})\} + [T][G]^{-1}\{A_s\}$$

$$[\overline{K}]\{A\} = \{\overline{F}(A_s, \mathbf{M})\}$$

Results of Field Simulations

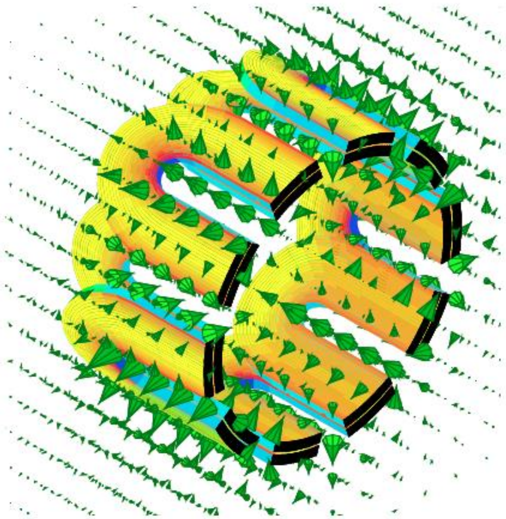

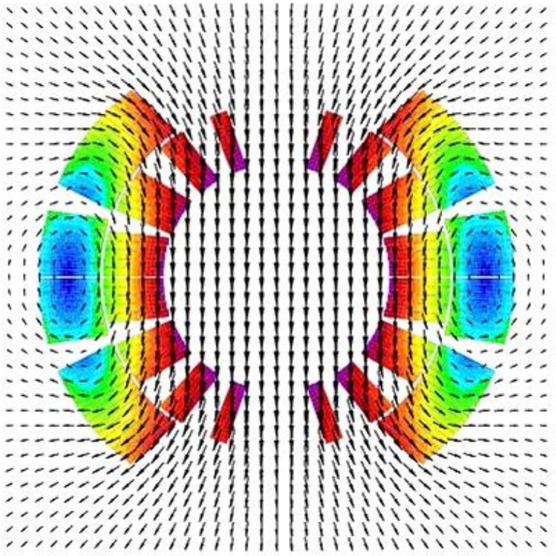

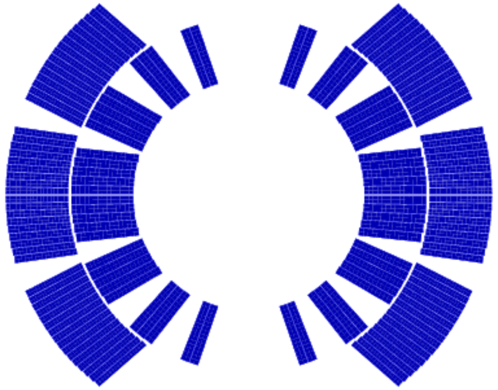

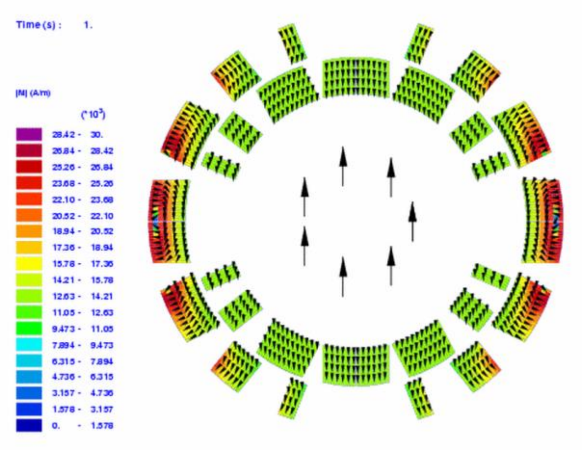

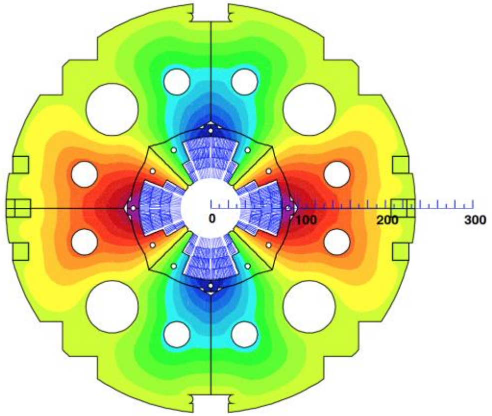

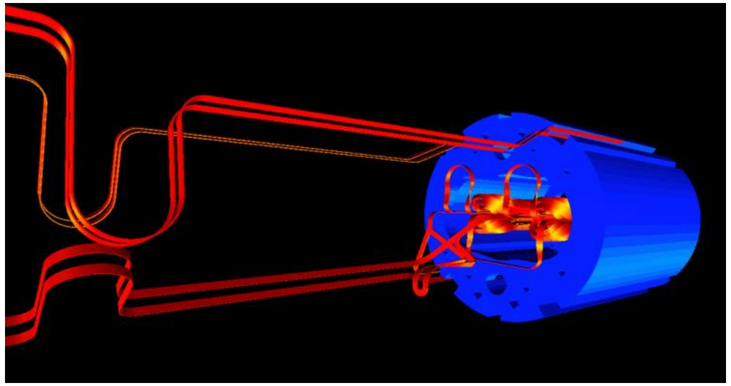

Limitations in numerical field simulation

- Intrinsic errors in model assumptions, partial physical model, off-nominal geometry (10 μm gap error = 10^{-4} field error)
- Approximation errors by the finite-element discretization, singularities at re-entrant corners
- Uncertainties on (inhomogeneous) material parameters, in particular for legacy equipment, martensitic phases, cold-working, stress-dependence
- Coupled phenomena such as magnetic, thermal, and mechanical effects, with extreme non-linearities in material parameters and varying time constants

- When numerical models fail to represent all physical properties of the magnets, a nonnegligible deviation is to be expected between model predictions and observations (measured data).

Example: Combined Function Magnets (CERN PS)

- Strongly coupled excitation circuits
- No 10^{-4} predictive model
- Remanent field ≈ 0.2%

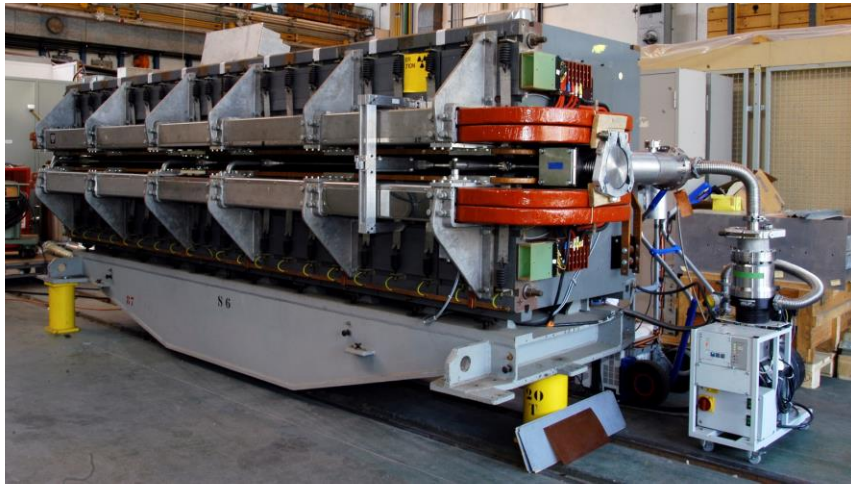

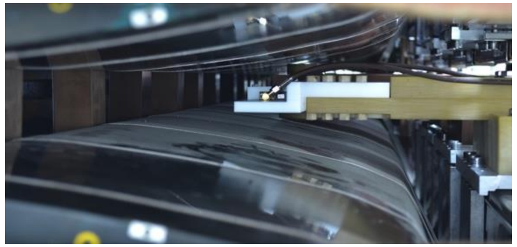

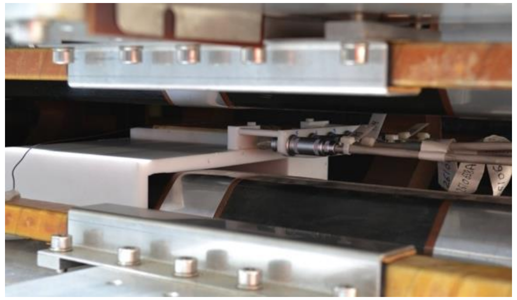

FMR field marker

Fluxmeter for gradient measureme

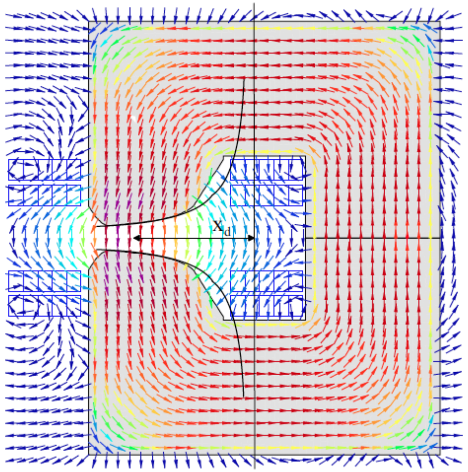

Figure-of-eight loop to control B_2, 4 pole face windings affecting B_1 to B_5

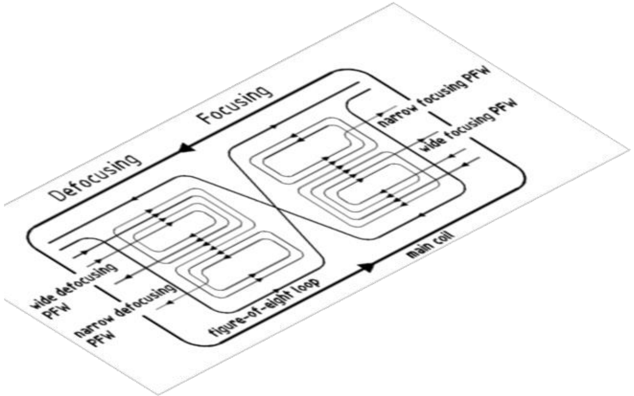

PS Beam Stability Test at Injection

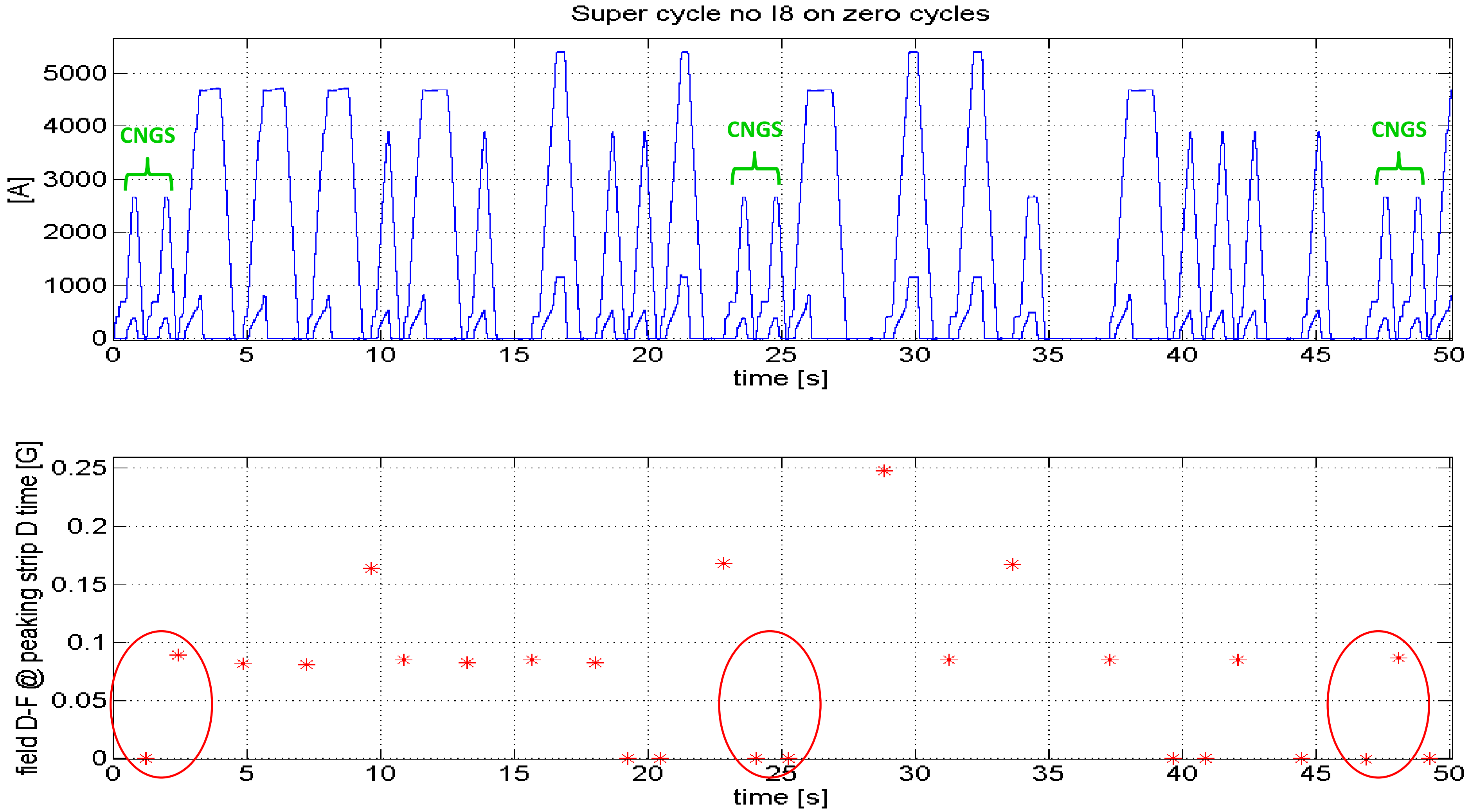

Specific powering cycles (CNGS) lead to reproducible radial positioning errors from relative field changes on the order of 10^{-5}

The Measurement Paradigm

- *Measurements on materials:* Hysteresis loops of highly permeable material both in DC and with controlled ramp, initial magnetization curve, critical current densities and magnetization in superconducting materials.
- *Measurements for design, prototype/pre-series:* Measuring material properties and validating design choices, validation of software and numerical models, prototype qualification
- *Measurements for magnet production:* Quality assurance and acceptance testing, magnet-to-magnet reproducibility, corrective actions (shimming), and requalification after repair, field quality of magnets “as built”.
- *Measurements for magnet-performance analysis:* Introspection, for example, computing peak fields and peak temperatures from models validated by global measurements of voltage decay curves during a magnet quench.
- *Measurements for accelerator operation*: Online monitoring of the field quality, field description and feed-forward compensation for a variety of excitation cycles.

Measured Quantities

- Material properties BH, coercitivity
- Integrated magnetic flux density
- Harmonic field content in 2D and 3D
- Magnetic-axis position
- Field angle
- V/I curve, differential inductance
- Decay time of ramp-induced eddy currents
- Transfer function of local or integrated fields versus excitation current
- Grid-based field maps of two or three field components at sampling points

Ring-Sample Permeameters

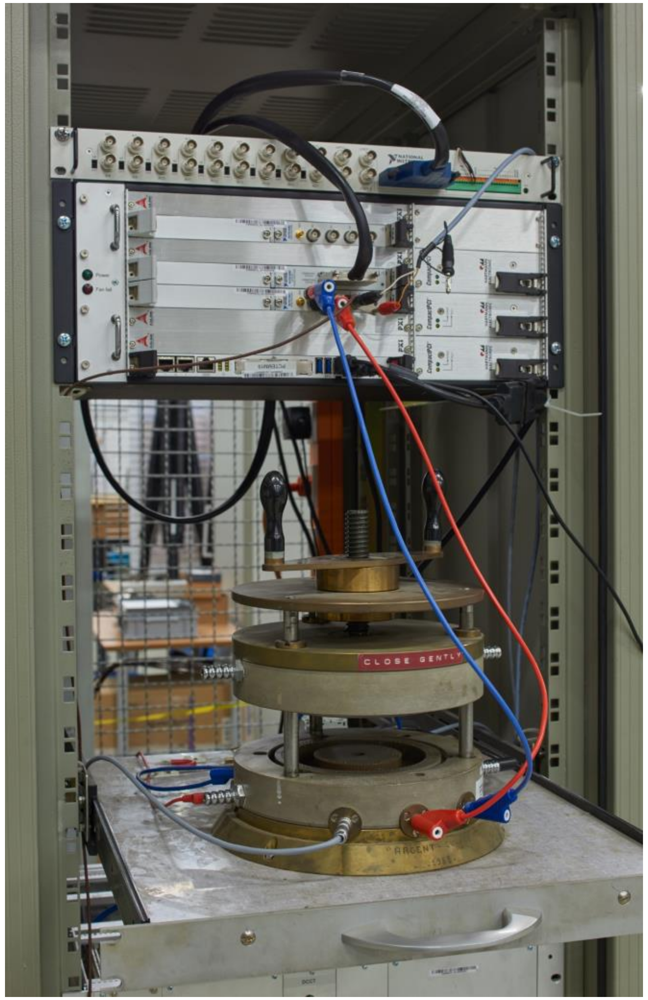

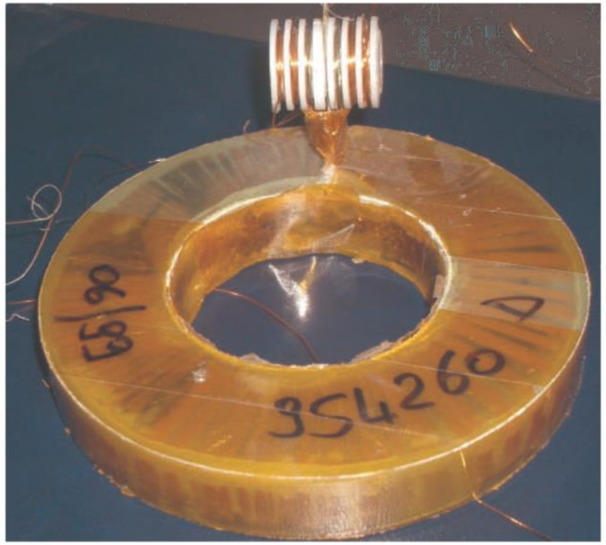

Temperature T	Stress	Coercive field H_c^B	Remanence B_r	max μ_r
K	MPa	$\mathrm{A\,m^{-1}}$	T	
300	0	68.4	1.07	5900
77	0	79.6	1.12	5600
4.2	0	85.1	1.06	4800
4.2	20	110	0.67	2460

Magnetic Measurement Systems (3D Hall Mapper)

3-axis precision stage

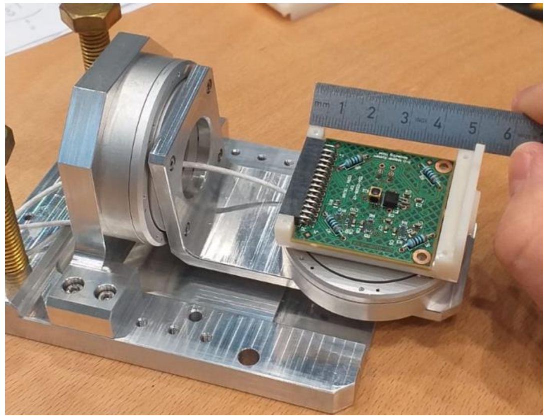

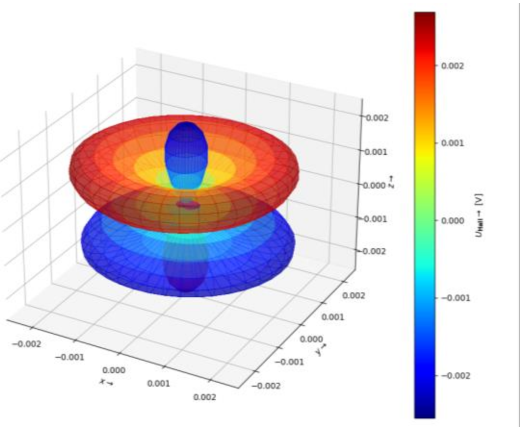

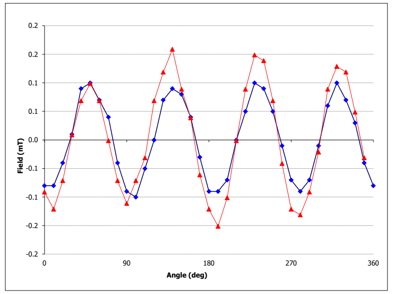

Rotating hall probe **polarity checker**
(high tolerance !)

Magnetic Measurement Systems (Stretched Wire)

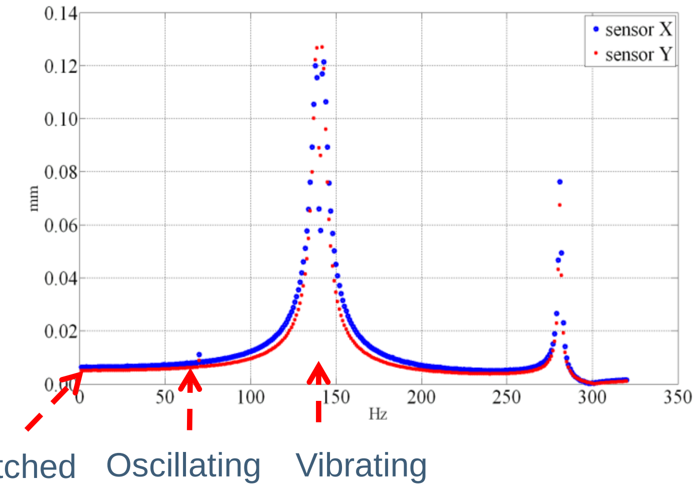

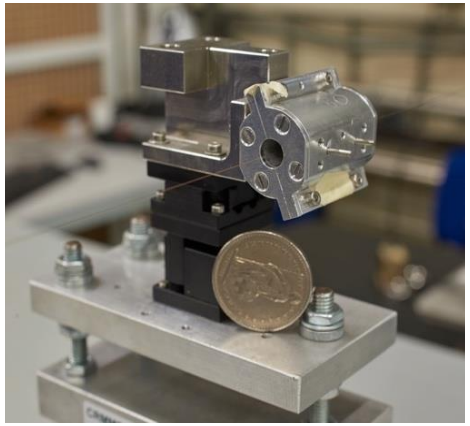

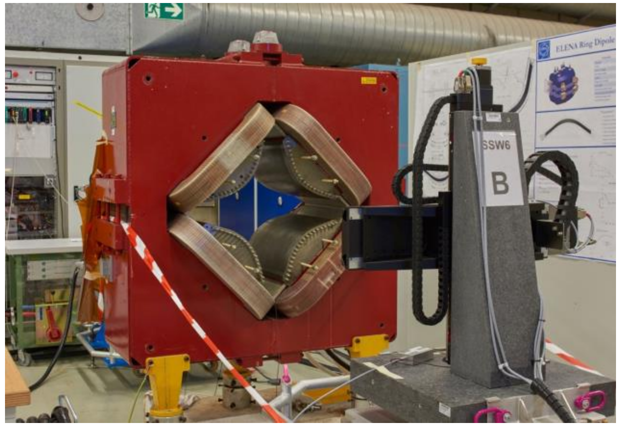

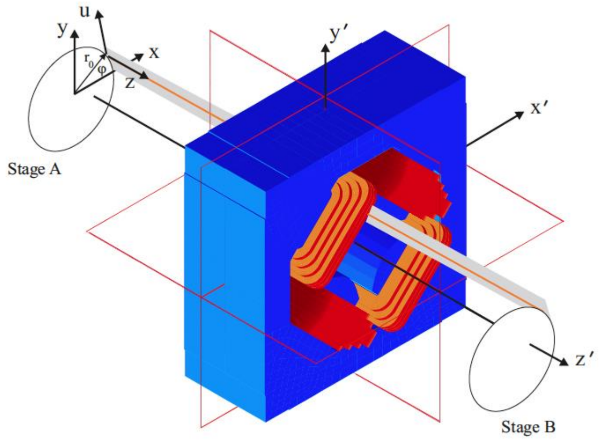

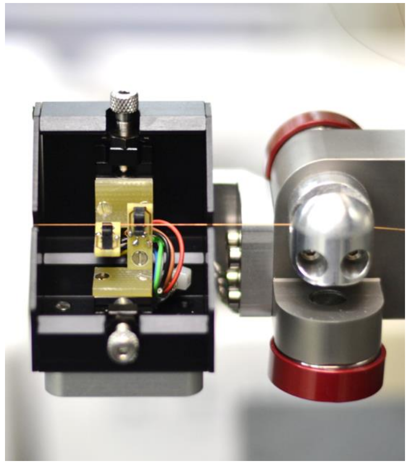

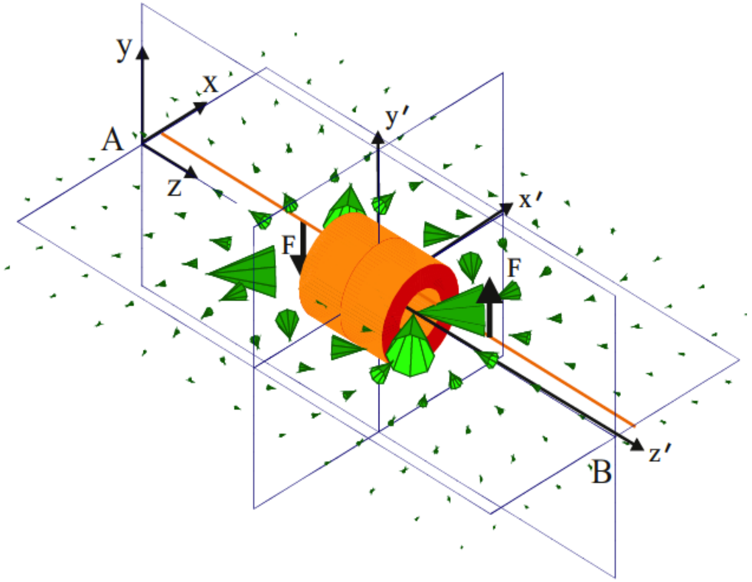

The Inhomogenous Wave Equation of the Taut String

$$u(x,t) = \sum_n \mathcal{U} \sin\left(\frac{n\pi}{L}z\right) \sin(\omega t - \varphi_n)$$

$$F(z,t) = -B_\mathrm{n}(z) I_0 \sin(\omega t)$$

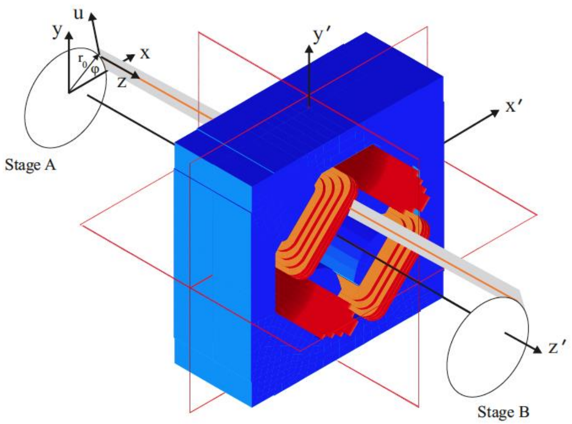

Lorentz Force Term on the Wire
Notice n = normal

$$\varphi_m = \arctan\left(\frac{\alpha\omega}{-\lambda_\mathrm{m}\omega^2 + T\left(\frac{m\pi}{L}\right)^2}\right)$$

Modal force

Nodal displacement

$$u(z,t) = \frac{2I_0}{L} \sum_m \frac{\int_0^L B_\mathrm{n}(z) \sin\left(\frac{m\pi}{L}z\right) \mathrm{d}z}{\sqrt{\left[T\left(\frac{m\pi}{L}\right)^2 - \lambda_\mathrm{m}\omega^2\right]^2 + (\alpha\omega)^2}} \sin\left(\frac{m\pi}{L}z\right) \sin(\omega t - \varphi_m)$$

Mode shape function

Numerical Simulation (FDTD) and the Steady State Solution

$$\frac{\partial^2 u}{\partial t^2}(t_i, z_n) \approx \frac{u(t_{i+1}, z_n) - 2u(t_i, z_n) + u(t_{i-1}, z_n)}{(\Delta t)^2} + O((\Delta t)^2),$$
$$\frac{\partial^2 u}{\partial z^2}(t_i, z_n) \approx \frac{u(t_i, z_{n+1}) - 2u(t_i, z_n) + u(t_i, z_{n-1})}{(\Delta z)^2} + O((\Delta z)^2).$$

$$u(t_i, z_{n+1}) = \sigma^2 u(t_i, z_{n+1}) + 2(1-\sigma^2) u(t_i, z_n) + \sigma^2 u(t_i, z_{n-1}) - u(t_{i-1}, z_n) - B_{\mathrm{n}}(z_n) I_0(t_i)$$

$$\sigma = \frac{c\Delta t}{\Delta z}$$

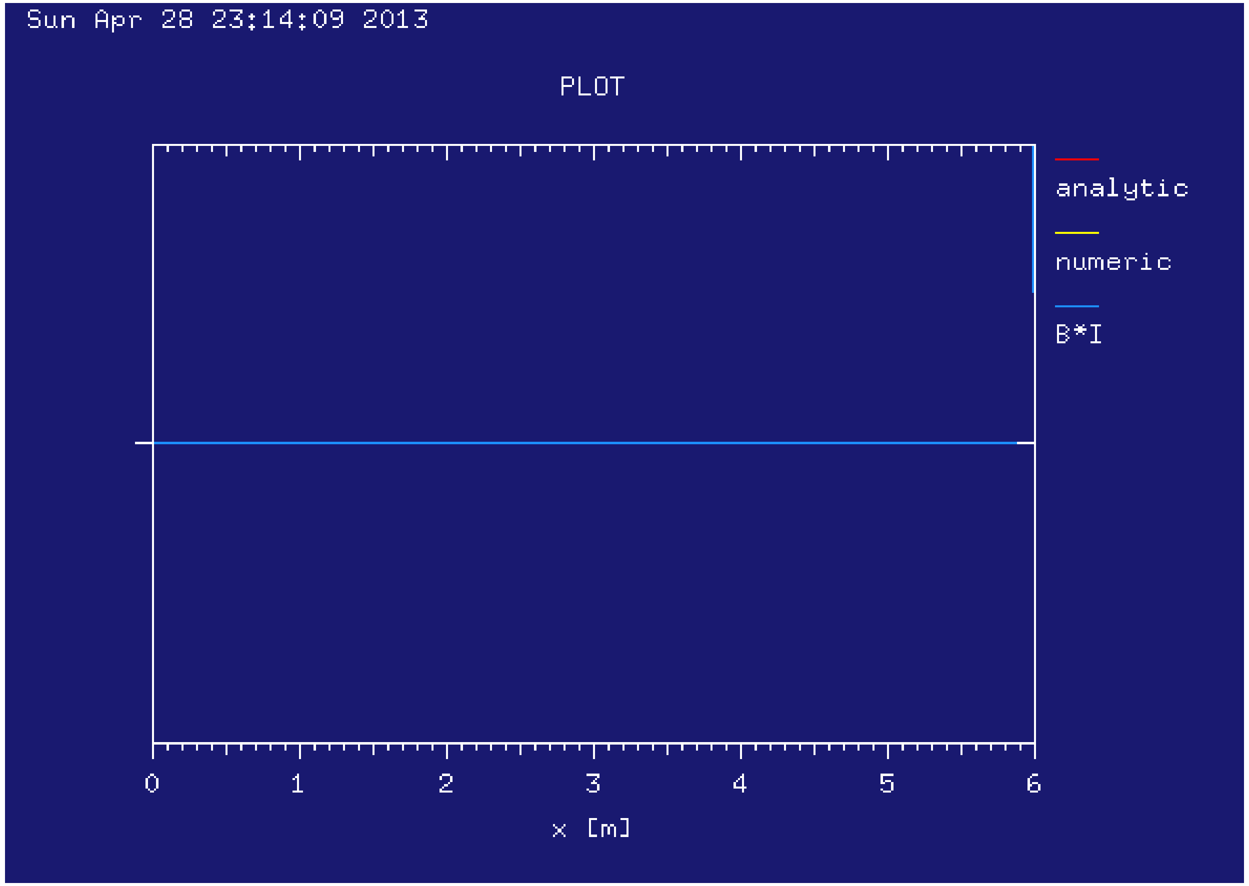

Magnetic Measurement Systems (induction-coil magnetometers)

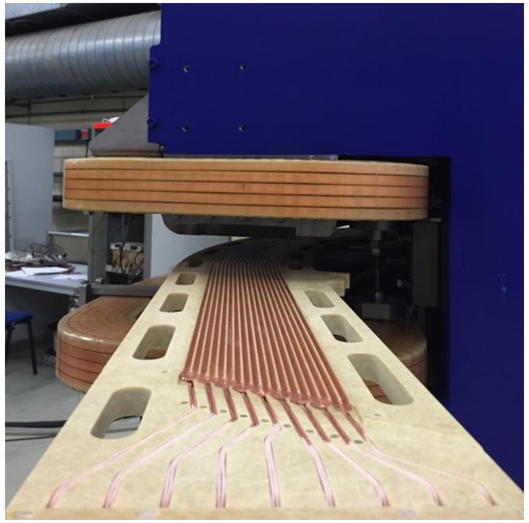

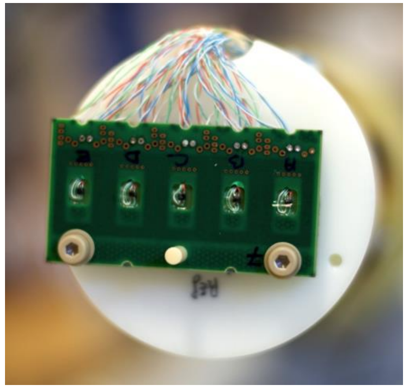

Stationary

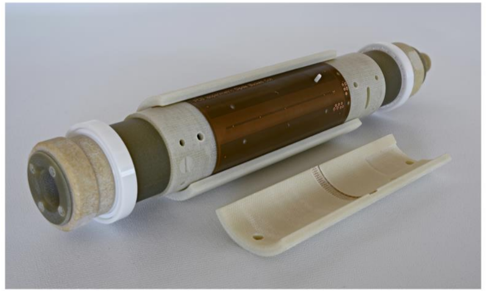

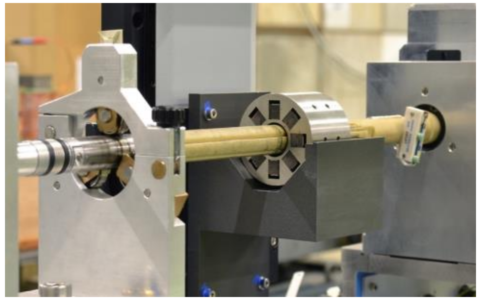

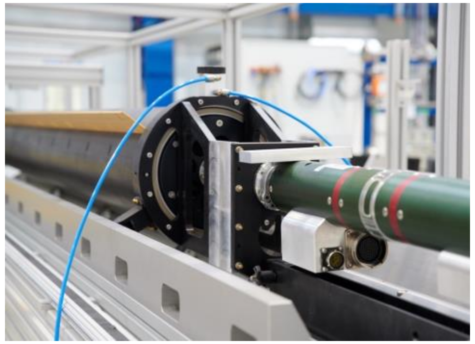

Rotational

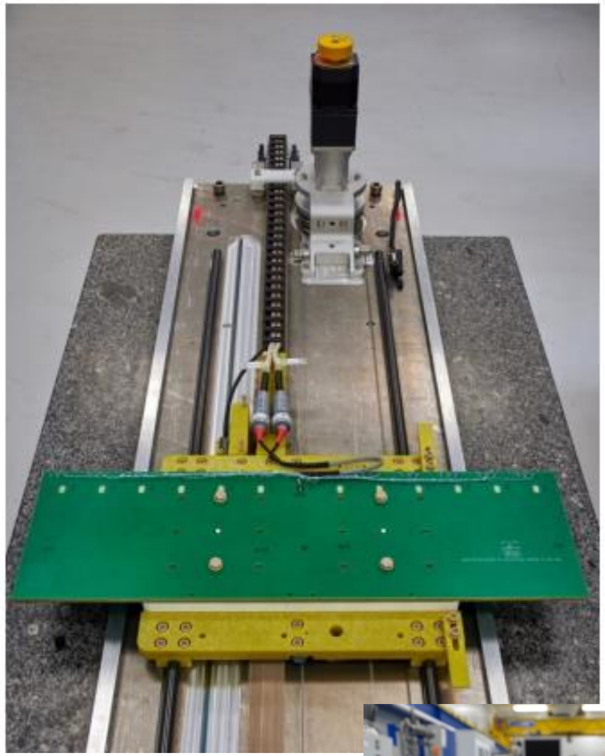

Translating

Rotating Coil Magnetometers

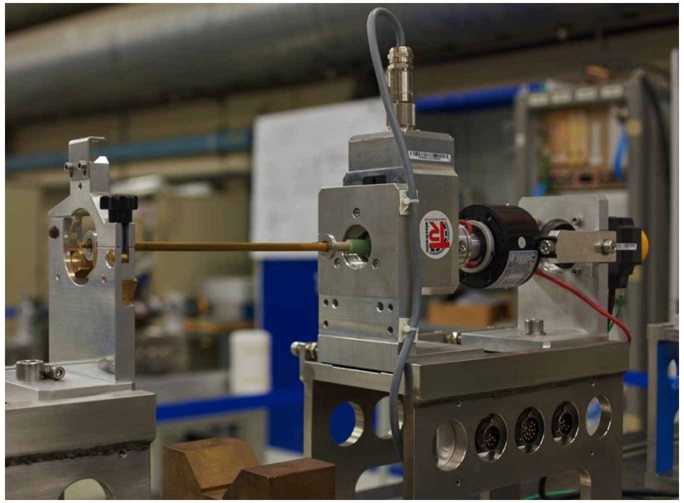

8 mm

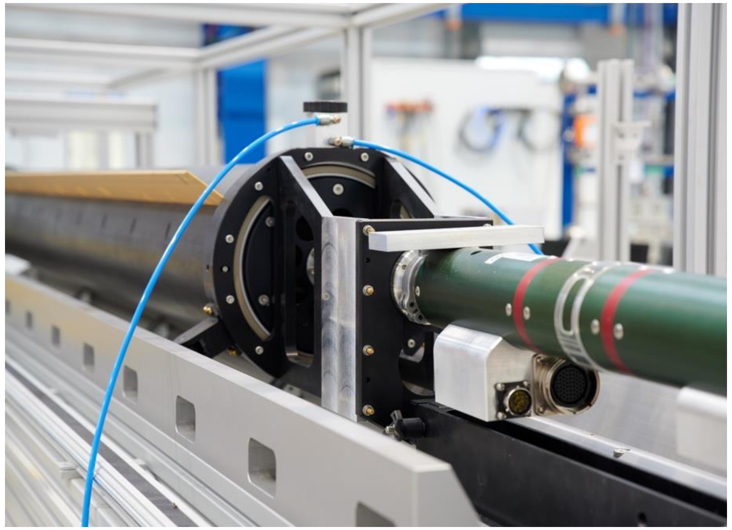

380 mm

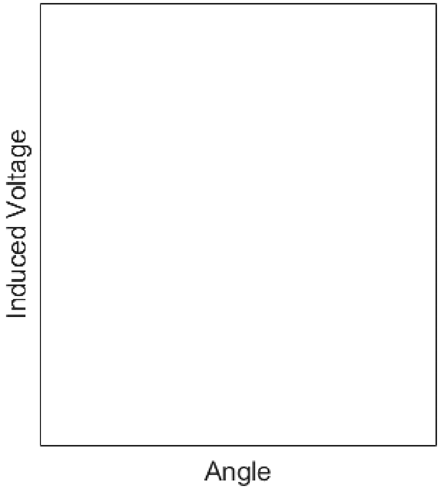

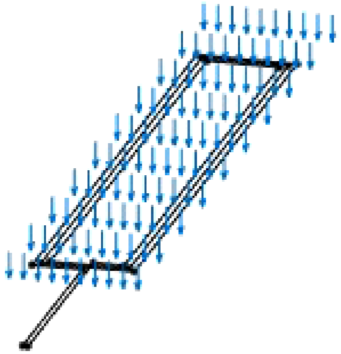

$$A_z(r,\varphi) = -\sum_{n=1}^{\infty} \frac{r_0}{n}\left(\frac{r}{r_0}\right)^n \left(B_n(r_0)\cos n\varphi - A_n(r_0)\sin n\varphi\right).$$

$$\Phi(\varphi) = \sum_{n=1}^{\infty} \frac{\ell}{r_0^{n-1}}\Big[K_n^{\mathrm{rad}}\,\left(B_n(r_0)\cos n\varphi - A_n(r_0)\sin n\varphi\right) + K_n^{\mathrm{tan}}\,\left(B_n(r_0)\sin n\varphi + A_n(r_0)\cos n\varphi\right)\Big]\,,$$

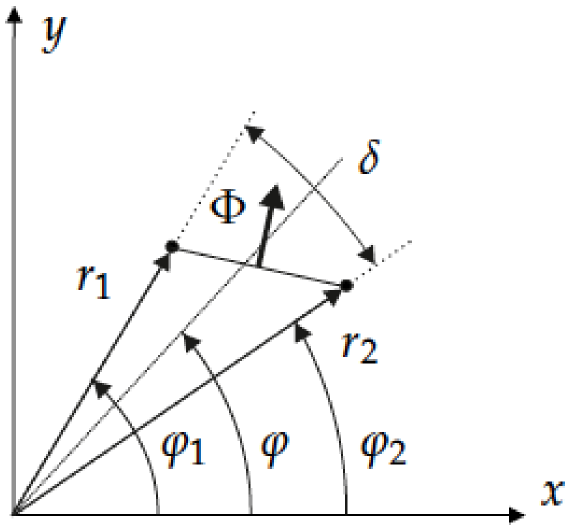

$$K_n^{\mathrm{rad}} = \frac{N}{n}\left[r_2^n\,\cos\,n(\varphi_2-\varphi) - r_1^n\,\cos\,n(\varphi_1-\varphi)\right],$$

$$K_n^{\mathrm{tan}} = -\frac{N}{n}\left[r_2^n\,\sin\,n(\varphi_2-\varphi) - r_1^n\,\sin\,n(\varphi_1-\varphi)\right],$$

Coil Calibration in CERN Reference Dipole

- Old CERN ISR bending dipole, cycled up to 1 T in a rigorously reproducible way
- Yearly mapping to establish field profile, averages and reproducibility
- We map By, but since the field is not perfectly uniform we have also Bx, Bz
  $\rightarrow$ the resulting (small) error is propagated to all instruments calibrated in this reference !

High precision NMR probe used to map the field

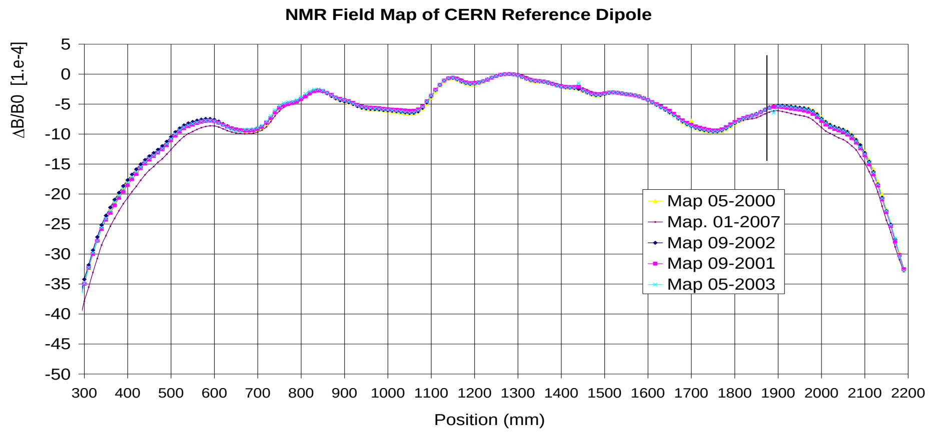

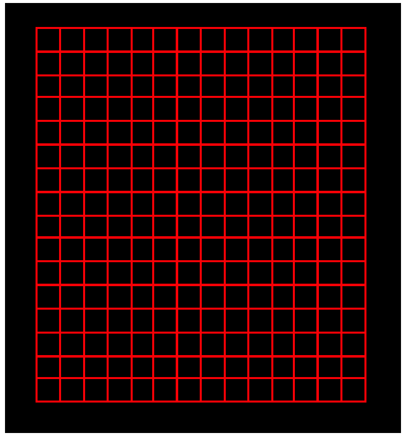

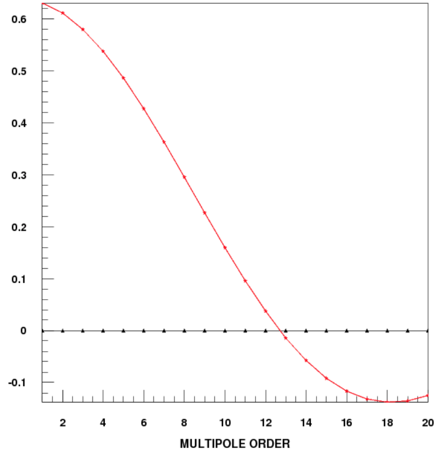

MULTIPOLE ORDER

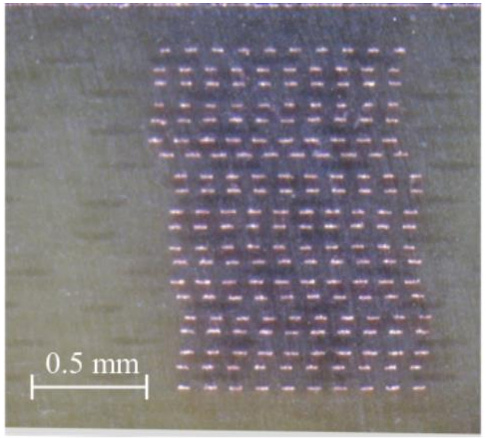

0.5 mm

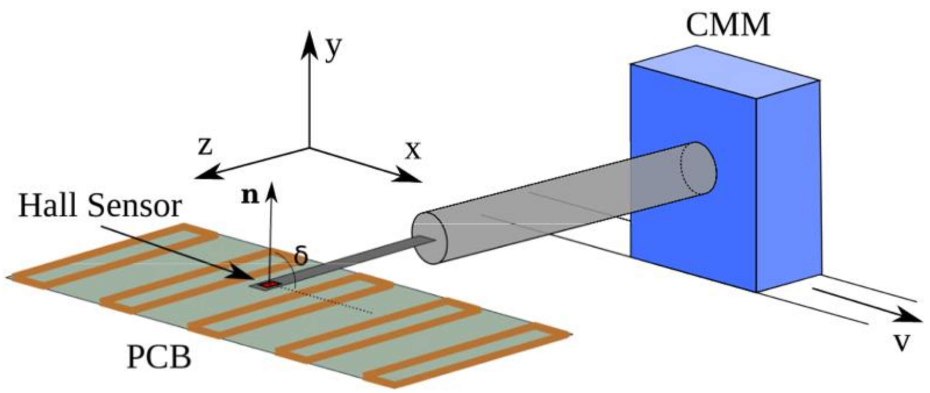

CMM
y
z
x
Hall Sensor
n
δ
PCB
v

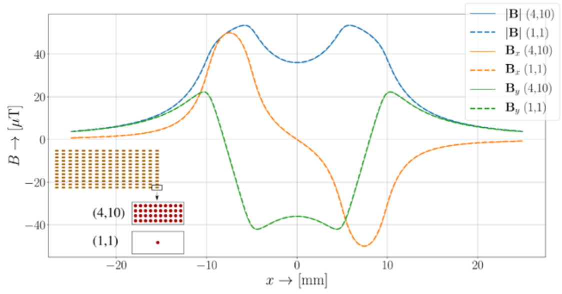

|B| (4,10)
|B| (1,1)
B_x (4,10)
B_x (1,1)
B_y (4,10)
B_y (1,1)
B → [μT]
x → [mm]
(4,10)
(1,1)

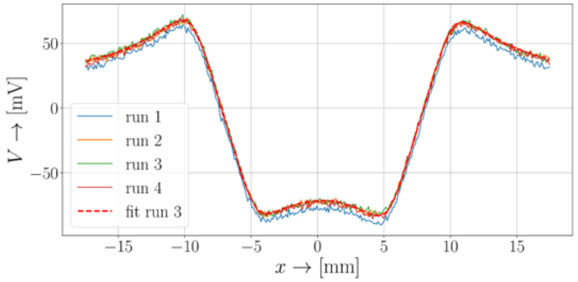

run 1
run 2
run 3
run 4
fit run 3
V → [mV]
x → [mm]

Rotating Coil Magnetometers in Use

Horizontal benches room temperature

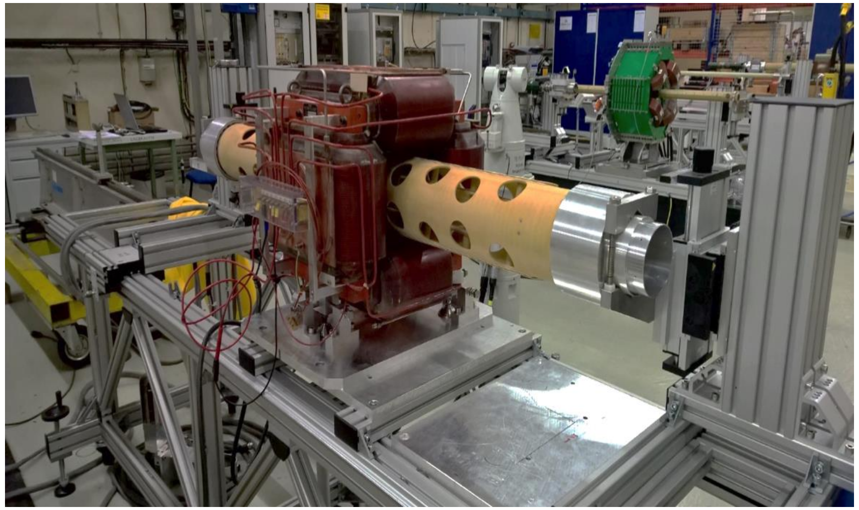

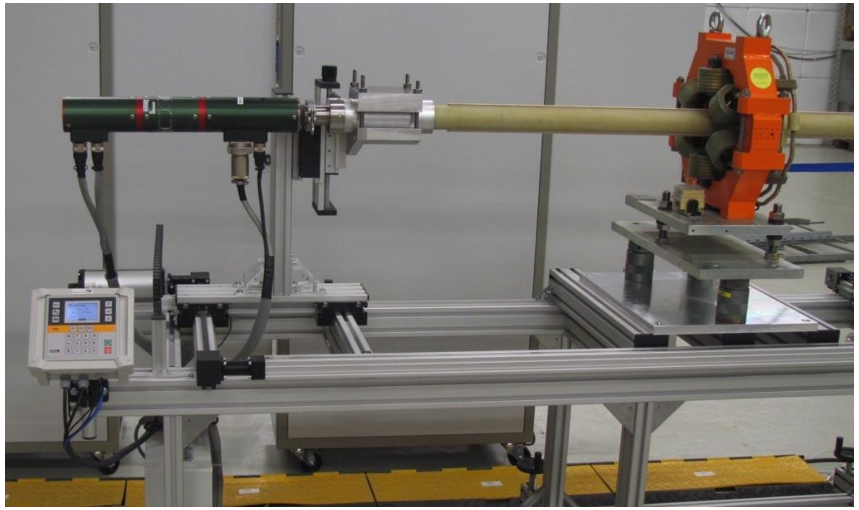

Vertical test station (cryogenic)

Solving the Boundary Value Problem (1)

1. Governing equation in the air domain $\nabla^2 A_z = 0,$

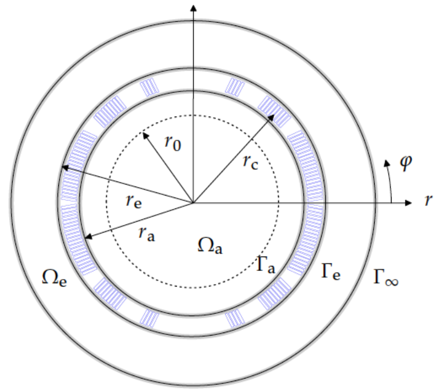

2. Chose a suitable coordinate system

$$r^2 \frac{\partial^2 A_z}{\partial r^2} + r \frac{\partial A_z}{\partial r} + \frac{\partial^2 A_z}{\partial \varphi^2} = 0,$$

3. Find eigenfunctions. Coefficients are not known

$$A_z(r,\varphi) = \sum_{n=1}^{\infty} r^n (\mathcal{A}_n \sin n\varphi + \mathcal{B}_n \cos n\varphi).$$

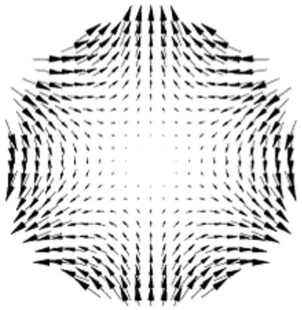

4. Calculate a field component

$$B_r(r,\varphi) = \frac{1}{r}\frac{\partial A_z}{\partial \varphi} = \sum_{n=1}^{\infty} n r^{n-1} (\mathcal{A}_n \cos n\varphi - \mathcal{B}_n \sin n\varphi),$$

5. Measure (or calculate) the field on a reference radius and perform Fourier analysis (develop into the eigenfunctions). Coefficients are known

$$B_r(r_0,\varphi) = \sum_{n=1}^{\infty} (B_n(r_0) \sin n\varphi + A_n(r_0) \cos n\varphi),$$

It also Works for the Integrated Fields (Potentials)

$$\overline{\phi}_{\mathrm{m}}(x,y) := \int_{-z_0}^{z_0} \phi_{\mathrm{m}}(x,y,z)\mathrm{d}z.$$

$$\nabla^2 \overline{\phi}_{\mathrm{m}}(x,y) = \frac{\partial^2 \overline{\phi}_{\mathrm{m}}(x,y)}{\partial x^2} + \frac{\partial^2 \overline{\phi}_{\mathrm{m}}(x,y)}{\partial y^2} = 0,$$

$$\begin{aligned}
\frac{\partial^2 \overline{\phi}_{\mathrm{m}}(x,y)}{\partial x^2} + \frac{\partial^2 \overline{\phi}_{\mathrm{m}}(x,y)}{\partial y^2} &= \int_{-z_0}^{z_0} \left(\frac{\partial^2 \phi_{\mathrm{m}}}{\partial x^2} + \frac{\partial^2 \phi_{\mathrm{m}}}{\partial y^2} \right) \mathrm{d}z \\
&= \int_{-z_0}^{z_0} \left(-\frac{\partial^2 \phi_{\mathrm{m}}}{\partial z^2} \right) \mathrm{d}z = - \left. \frac{\partial \phi_{\mathrm{m}}}{\partial z} \right|_{-z_0}^{z_0} \\
&= H_z(-z_0) - H_z(z_0) \stackrel{!}{=} 0\,.
\end{aligned}$$

Local Field Distribution (Fourier-Bessel Series)

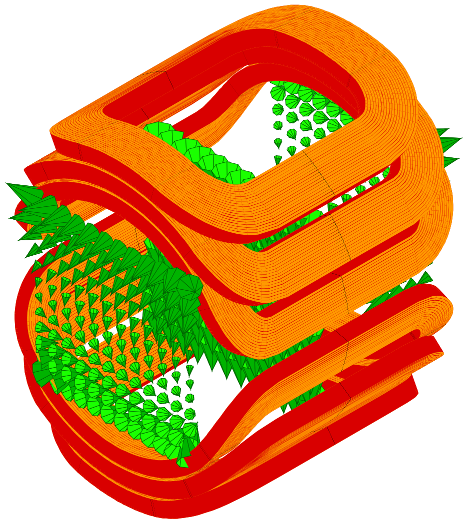

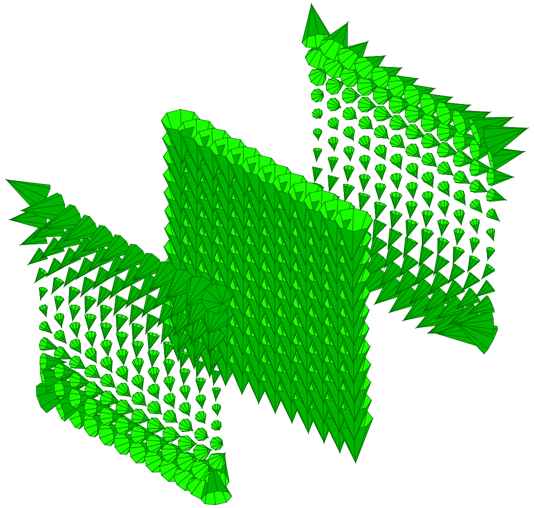

$$\phi_{\mathrm{m}}(r,\varphi,z) = \left\{ \begin{array}{c} \cos n\varphi \\ \sin n\varphi \end{array} \right\} I_n(pr) \left\{ \begin{array}{c} \cos pz \\ \sin pz \end{array} \right\}$$

$$\begin{aligned}
\phi_{\mathrm{m}} = \sum_{n=1}^{\infty} \Big\{ & \mathcal{C}_{n,n}(z) - \frac{\mathcal{C}_{n,n}^{(2)}(z)}{4(n+1)} r^2 \\
& + \frac{\mathcal{C}_{n,n}^{(4)}(z)}{32(n+1)(n+2)} r^4 - \frac{\mathcal{C}_{n,n}^{(6)}(z)}{384(n+1)(n+2)(n+3)} r^6 + \dots \Big\} r^n \sin n\varphi \\
+ \sum_{n=1}^{\infty} \Big\{ & \mathcal{D}_{n,n}(z) - \frac{\mathcal{D}_{n,n}^{(2)}(z)}{4(n+1)} r^2 \\
& + \frac{\mathcal{D}_{n,n}^{(4)}(z)}{32(n+1)(n+2)} r^4 - \frac{\mathcal{D}_{n,n}^{(6)}(z)}{384(n+1)(n+2)(n+3)} r^6 + \dots \Big\} r^n \cos n\varphi \,,
\end{aligned}$$

Short Induction Coils Must be Isoperimetric

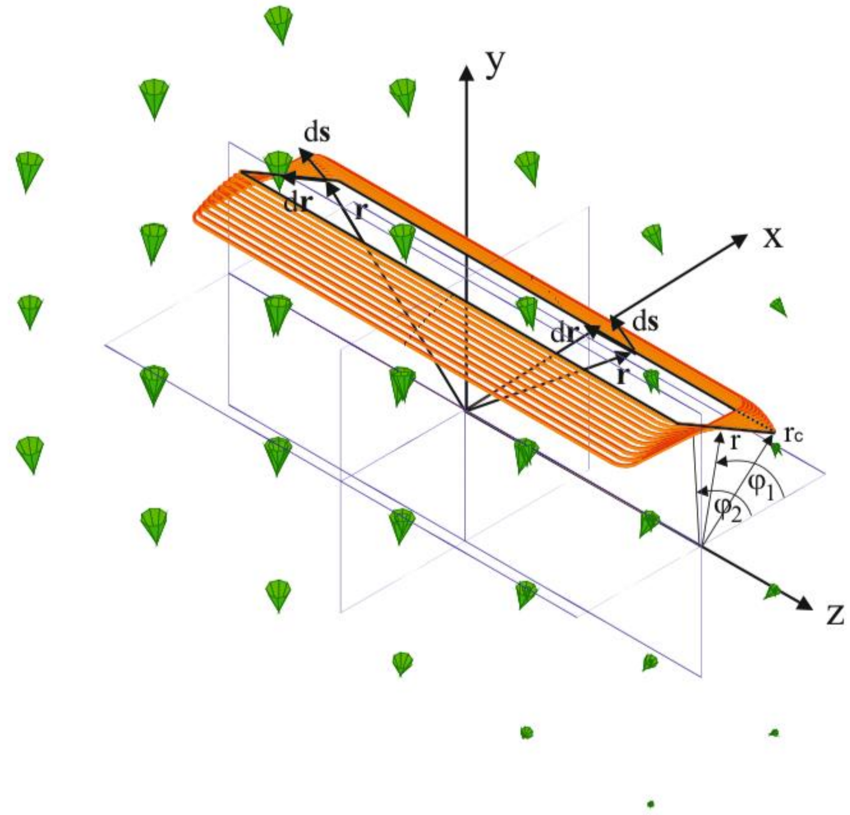

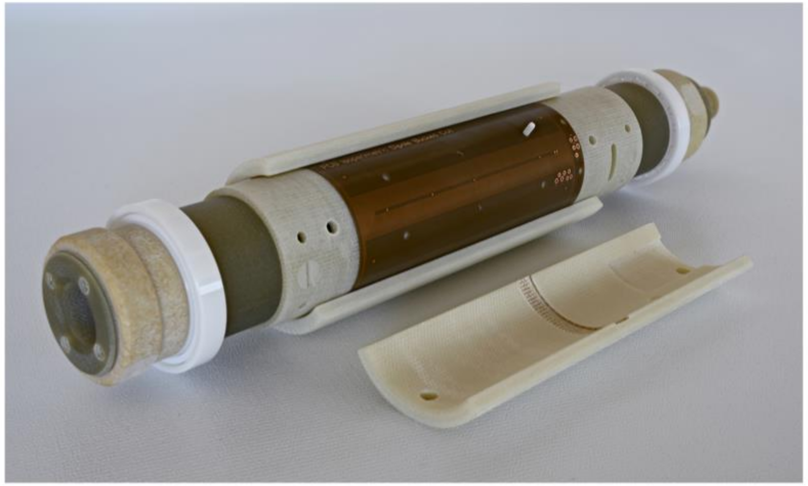

The Leading Term is NOT the Measured One

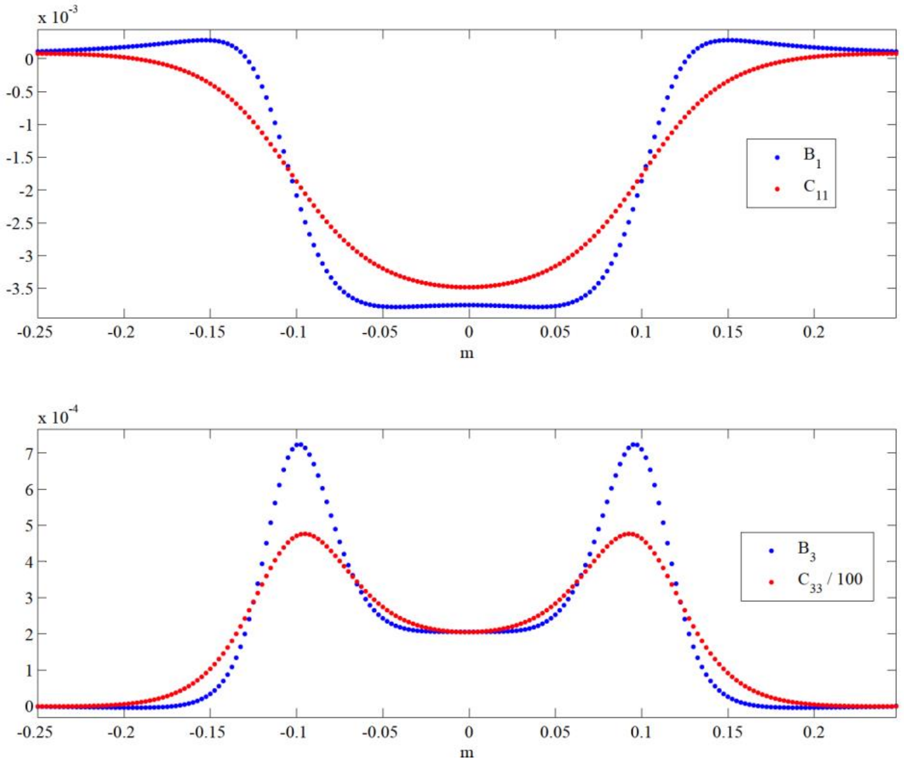

$$B_n(r_0, z) = -\mu_0\, r_0^{n-1} \overline{\mathcal{C}}_n(r_0, z) =$$

$$-\mu_0\, r_0^{n-1} \left(n\, \mathcal{C}_{n,n}(z) - \frac{(n+2)\mathcal{C}_{n,n}^{(2)}(z)}{4(n+1)} r_0^2 + \frac{(n+4)\mathcal{C}_{n,n}^{(4)}(z)}{32(n+1)(n+2)} r_0^4 - \dots \right) .$$

Translating Induction-Coil Magnetometers (planar)

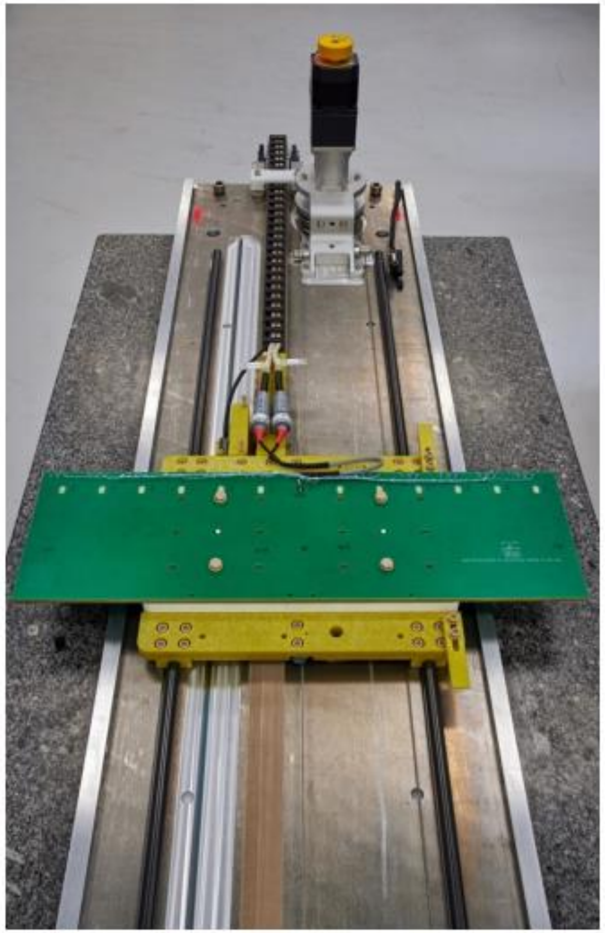

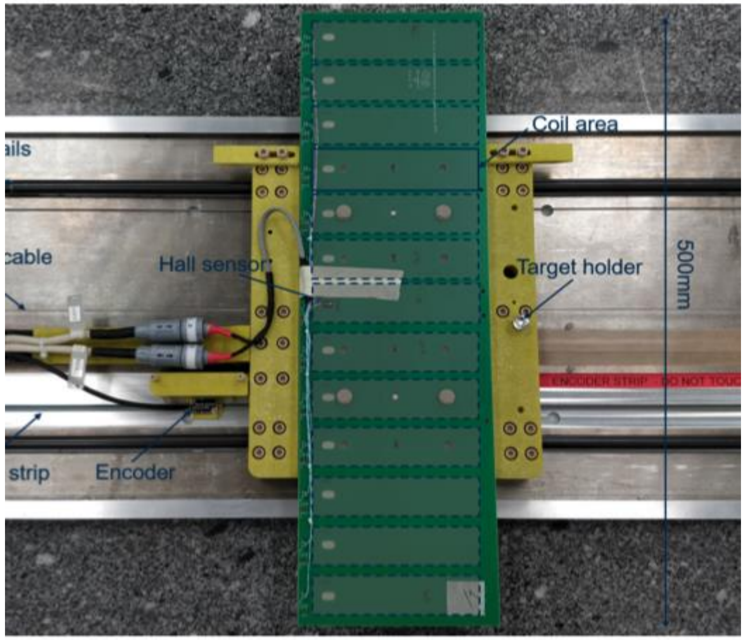

For FAIR

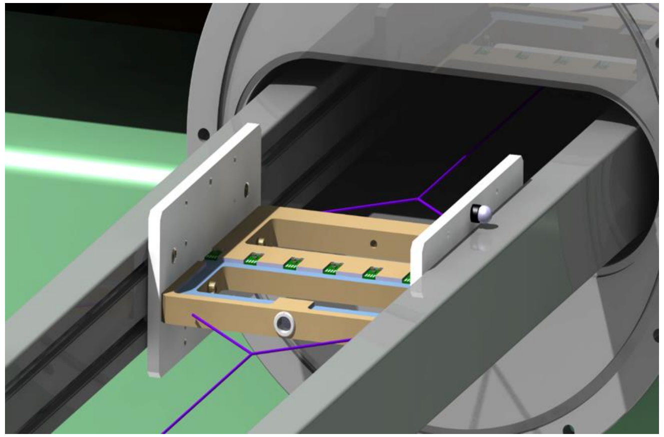

For NA64

Mid-Plane Field Development

$$
\begin{aligned}
\frac{-1}{\mu_0} B_y(x, y=0, z) \approx \\
& \mathcal{C}_{1,1}(z) - \frac{\mathcal{C}_{1,1}^{(2)}(z)}{8} x^2 + \frac{\mathcal{C}_{1,1}^{(4)}(z)}{192} x^4 - \frac{\mathcal{C}_{1,1}^{(6)}(z)}{9216} x^6 \\
& + 3\,\mathcal{C}_{3,3}(z)\, x^2 - \frac{3\,\mathcal{C}_{3,3}^{(2)}(z)}{16} x^4 + \frac{3\,\mathcal{C}_{3,3}^{(4)}(z)}{640} x^6 \\
& + 5\,\mathcal{C}_{5,5}(z)\, x^4 - \frac{5\,\mathcal{C}_{5,5}^{(2)}(z)}{24} x^6 \\
& + 7\,\mathcal{C}_{7,7}(z)\, x^6
\end{aligned}
$$

Translating Induction-Coil Magnetometers (solenoidal)

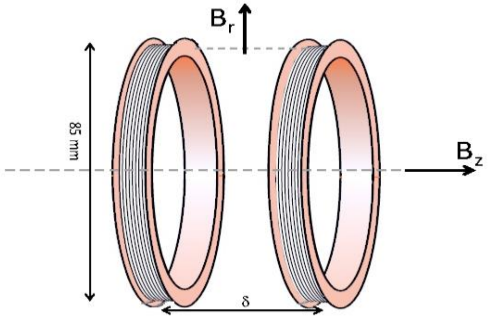

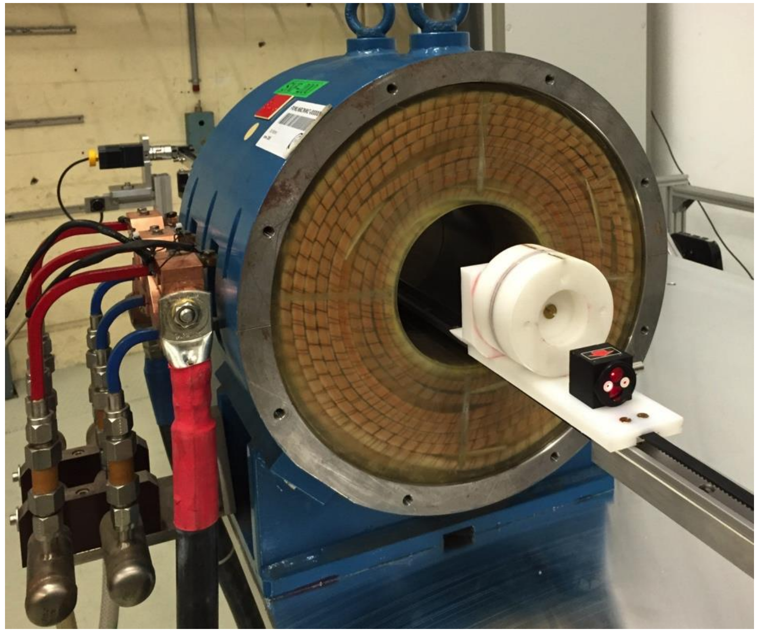

$$B_z(r,z) = -\mu_0 \left(\mathcal{C}_{0,0}^{(1)}(z) - \frac{\mathcal{C}_{0,0}^{(3)}(z)}{4} r^2 + \frac{\mathcal{C}_{0,0}^{(5)}(z)}{64} r^4 \right) \qquad B_r(r,z) = -\mu_0 \left(-\frac{\mathcal{C}_{0,0}^{(2)}(z)}{2} r + \frac{\mathcal{C}_{0,0}^{(4)}(z)}{16} r^3 \right)$$

$$\mathcal{F}\{B_r(r_0,z)\} = -\mu_0\, \mathcal{F}\{\mathcal{C}_{0,0}(z)\} \left(-\frac{(i\omega)^2}{2} r_0 + \frac{(i\omega)^4}{16} r_0^3 \right)$$

Limitations in Magnetic Measurements

- ➔ Random errors such as capture and read-out noise
- ➔ Systematic errors from voltage dividers, calibration, inexact values of standards and references, integrator drift, or stray fields
- ➔ Operator errors, for example, using the wrong calibration data or relying on outdated scripts for postprocessing
- ➔ Approximation errors from the projection of measurement data onto Fourier polynomials
- ➔ Intrinsic errors from (false) assumptions of linearity of the sensor response or non-orthogonal sensors
- ➔ Inadequate knowledge of the effects of environmental conditions
- ➔ Ignorance (unrecognized systematic effects) from model reduction, such as neglecting mechanical and thermal effects, access constraints (e.g. in strongly curved or magnets installed in the accelerator), or non-availability to reproduce operational powering cycles in the measurement lab

Reducing the Uncertainty in Magnetic Measurements

- Stable mechanics – vibration reduction
- Precise positioning (distance (relative) better then position (absolute))
- Low noise environment (ground motion, EMC, temperature)
- Re-parametrization to arc-length
- Compensation of main signals (bucking)
- Calibration, cross-calibration (in situ), and traceability of results
- Making use of symmetry (flip and repeat, reverse polarity)
- Repetition (average random errors)
- Oversampling
- Low-pass filtering and integration (drift compensation)
- Using the regularity conditions of magnet fields
  - Feed-down corrections
  - Developing into orthogonal eigenfunctions
  - Boundary-element postprocessing

Reparametrization to Arc Length

$$
\begin{aligned}
\int_{t_1(s_1)}^{t_2(s_2)} U(\partial\mathscr{A}) \cdot \mathrm{d}t &= \int_{t_1(s_1)}^{t_2(s_2)} \int_{\partial\mathscr{A}} (\mathbf{v}_\mathrm{p} \times \mathbf{B}) \cdot \mathrm{d}\mathbf{r}\, \mathrm{d}t \\
&= \int_{t_1(s_1)}^{t_2(s_2)} \int_{\partial\mathscr{A}} -\mathbf{B} \cdot (\mathbf{v}_\mathrm{p} \times \mathrm{d}\mathbf{r}) \mathrm{d}t \\
&= \int_{t_1(s_1)}^{t_2(s_2)} \int_{\partial\mathscr{A}} -\mathbf{B} \cdot (\mathbf{v}_\mathrm{p} \mathrm{d}t) \times \mathrm{d}\mathbf{r} \\
&= \int_{\partial\mathscr{A}} \int_{s_1}^{s_2} -\mathbf{B} \cdot (\mathrm{d}\mathbf{s} \times \mathrm{d}\mathbf{r}) \\
&= \int_{\mathscr{A}_\mathrm{s}} -\mathbf{B} \cdot \mathrm{d}\mathbf{a}\,,
\end{aligned}
$$

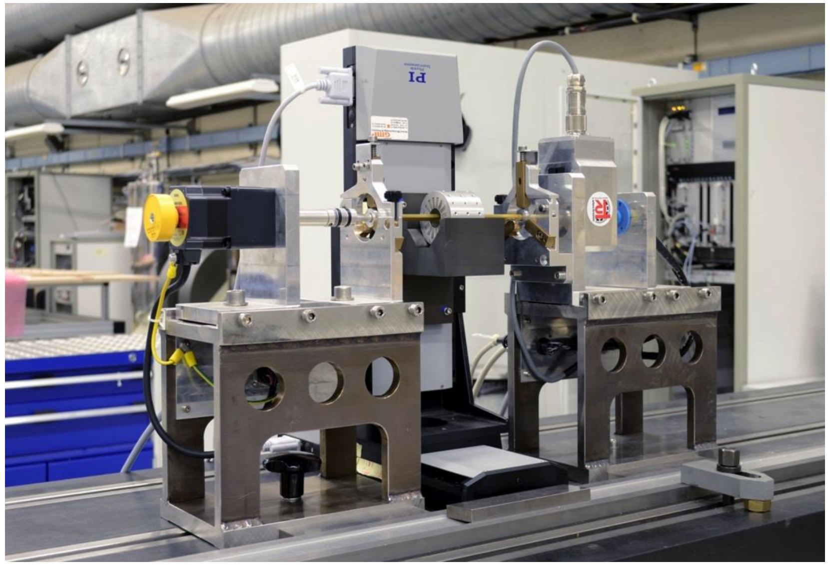

Low drift, low-noise amplifier = resolution of 10 nVs

One cycle = 1 – 10 s

1024 trigger points for discrete Fourier transform

In-Situ Cross-Calibration

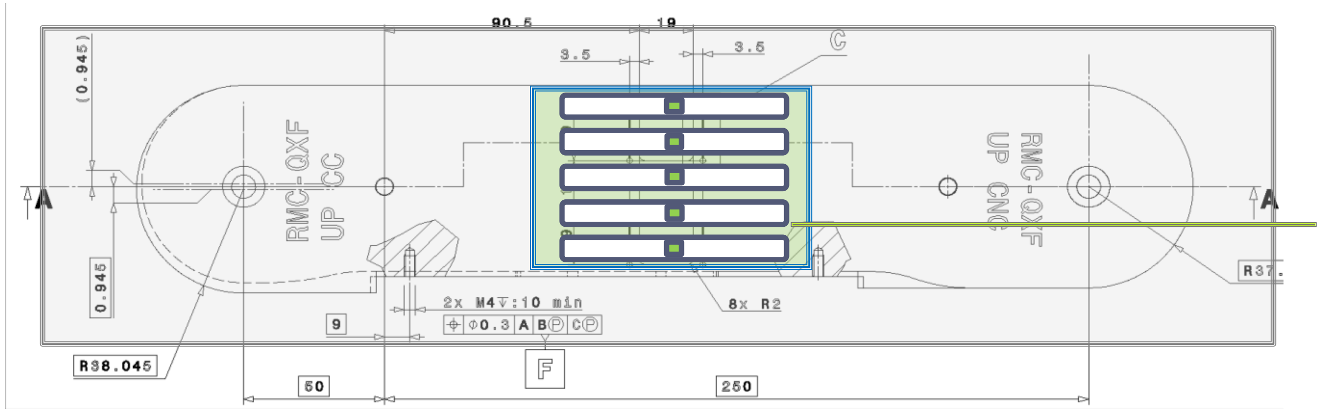

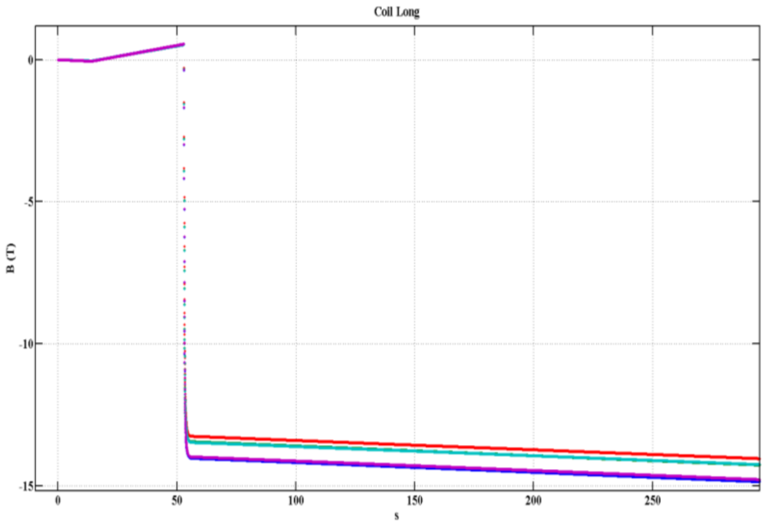

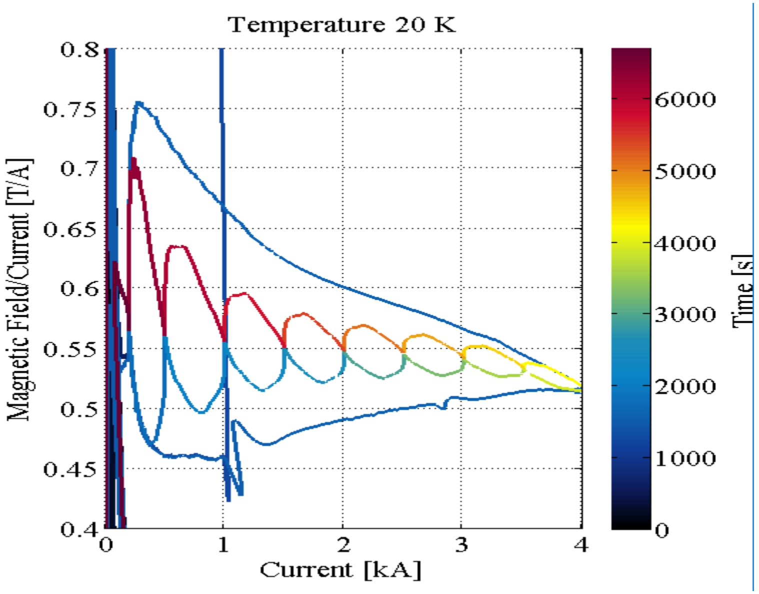

Integrator drift: 0.5% over 60 s on average

Uncertainty Mitigation Measures (Systematic Errors and Gross Errors)

- Calibration: to establish the transfer function of a given instrument by comparison with a reference instrument of known accuracy
  - cross-checks with instruments of comparable uncertainty to gain confidence or eliminate gross errors
  - in-situ calibration: use the magnet to be tested as the reference via a previous measurement with a reference instrument

- Traceability: an unbroken chain of comparisons, each with a stated uncertainty, from a measurement to a primary standard.
  - Fundamental concept to certify a measurement; maintaining systematic records, databases, documented procedures

The Problem Setting

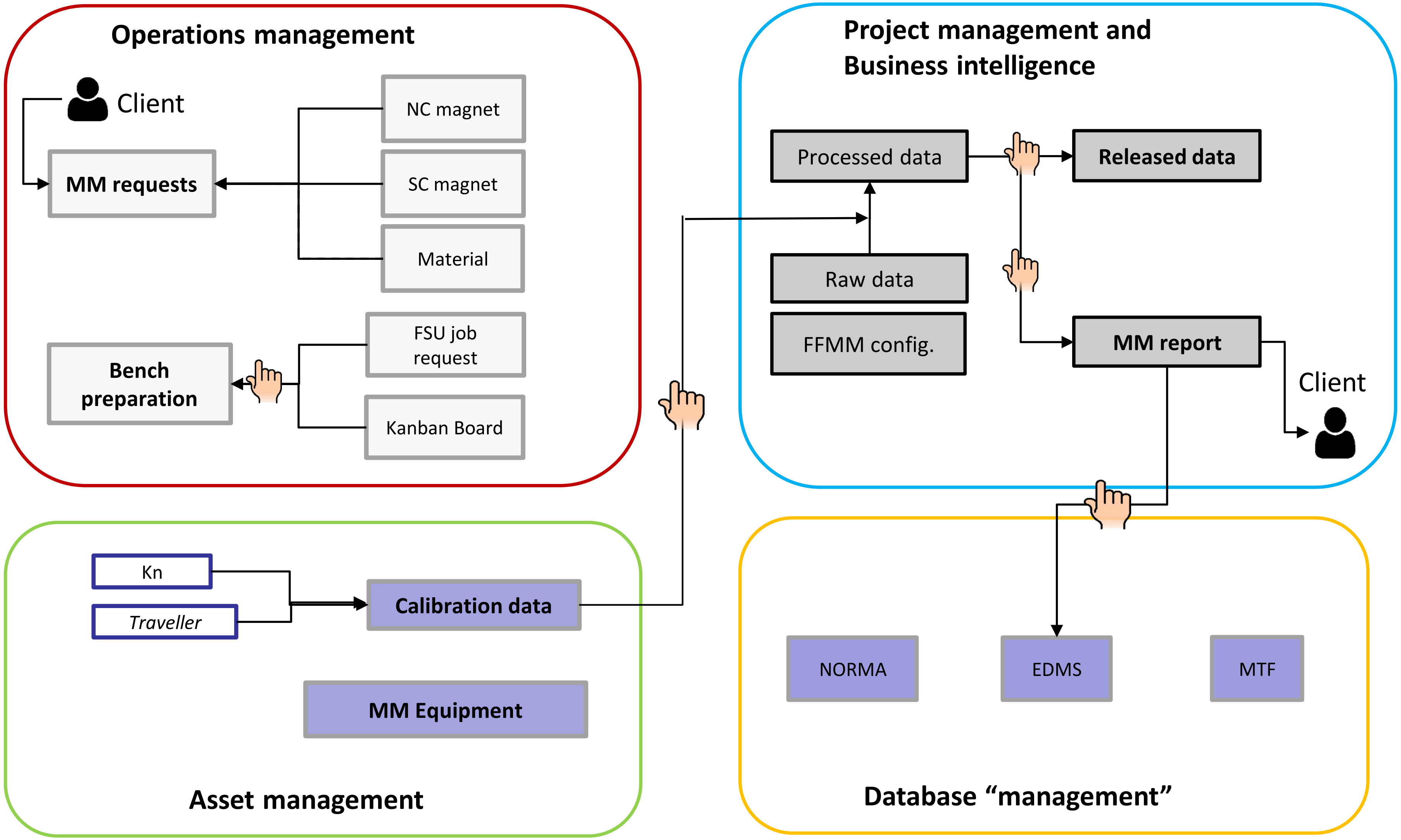

Database and Asset Management integrated with Control and DAQ

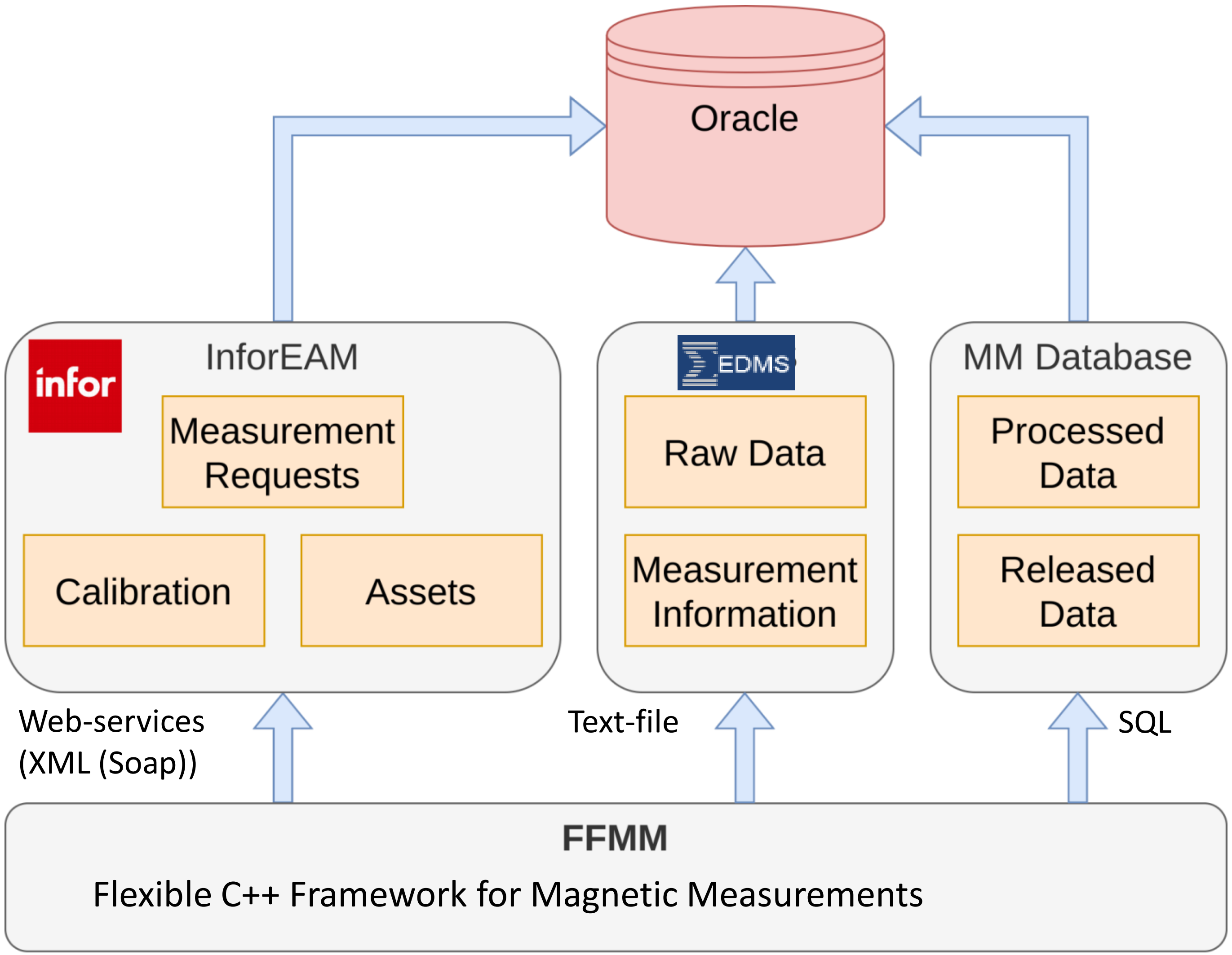

The Avatar and Twin (classical black-box measurement)

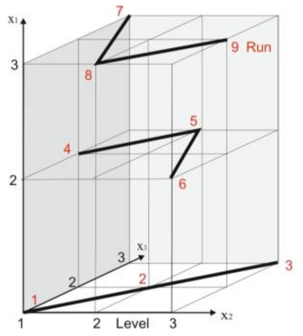

Physical object (magnet)

Magnetic flux density in the magnet bore

Capture noise

Parameters

Field Transducer

Read-out noise

Design of experiment
Taguchi array testing

Raw signal (voltages)

AD-conversion
Digital integration,
Drift correction

Processed data (fluxes)

Modelling,
Calibration,
Approximation errors

$$B_n(r_0) \approx \frac{2}{K}\sum_{k=1}^{K} B_r(r_0,\varphi_k)\sin n\varphi_k.$$

The Avatar and Twin (generalized field description with updated model)

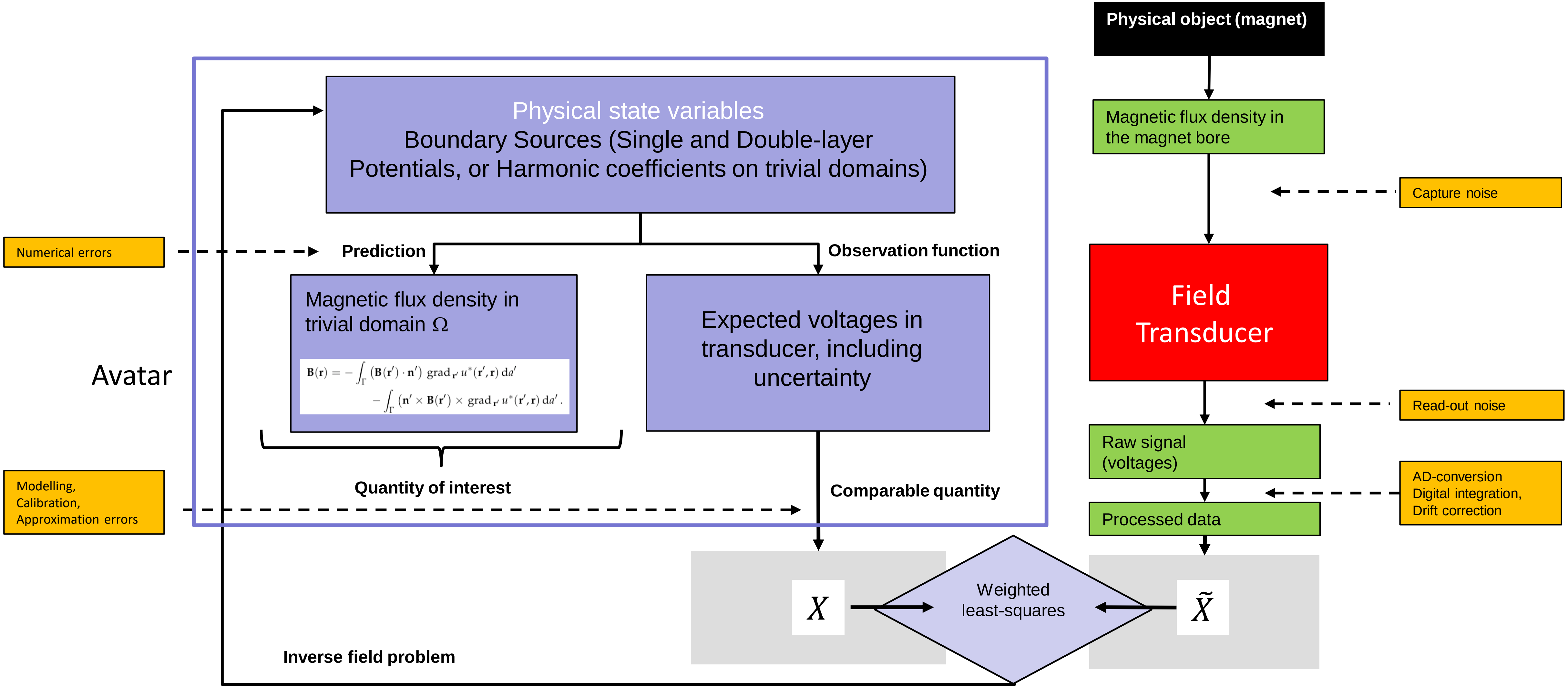

Sensitivity included in Observation Function (not in MM Post-Processing)

➔ The **observation function** $s\colon \boldsymbol{B}(\boldsymbol{r},t) \to U(\boldsymbol{r},t)$ is determined by modelling the magnetic measurement technique which allows including calibration and the sources of uncertainty:

- Modelling errors (neglect of temperature dependent
- Approximation errors (coil parameters approximated by surface and radius)
- Calibration errors (e.g., errors in the surface and radius measurements)

➔ The inverse observation function $s^{-1}\colon U(\boldsymbol{r},t) \to \boldsymbol{B}(\boldsymbol{r},t)$ may **not** exist

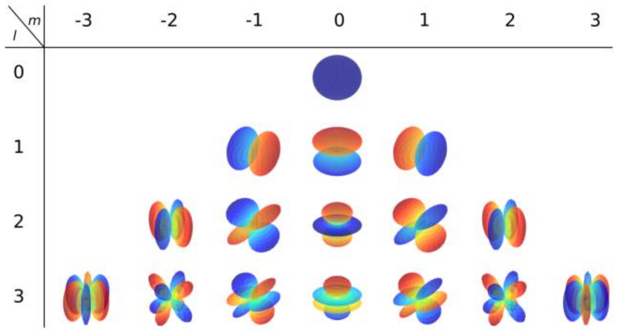

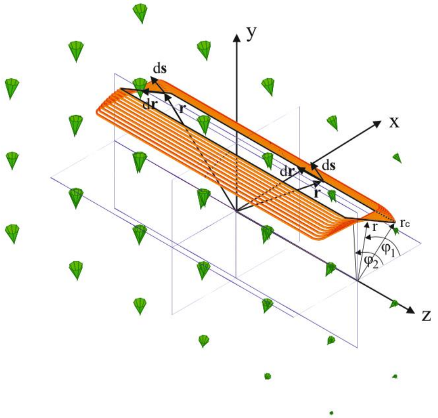

Coil couples with B_r and B_z

➔ The observation function allows the combination of different transducers (sensor fusion)

Example: 2D Integrated Field Reconstruction by Rotating Coil Mapping

Physical object (magnet)

Magnetic flux density in the magnet bore

Capture noise

Huron bench

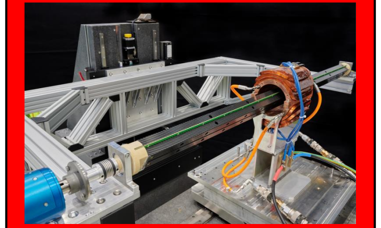

Read-out noise

Raw signal (voltages)

AD-conversion
Digital integration,
Drift correction

Harmonics

Magnetic field parameterized by multipole coefficients in large magnet aperture

$$A_z(r,\varphi) = \sum_{n=1}^{\infty} r^n (\mathcal{A}_n \sin n\varphi + \mathcal{B}_n \cos n\varphi).$$

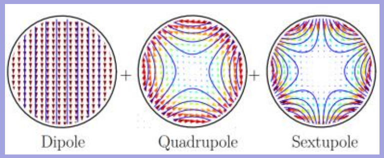

Numerical errors

Prediction

Observation function
Feed-Down Formula

Field Quality

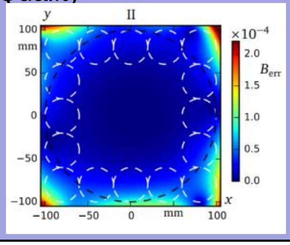

Off-centered multipoles

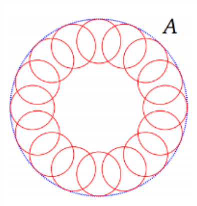

$$C_n'(r_c, z_i) = \sum_{k=n}^{K} C_k(r_0, z_0) \binom{k-1}{k-n} \left(\frac{z_i}{r_0}\right)^{k-n} \left(\frac{r_c}{r_0}\right)^{n-1}$$

Quantity of interest

Coil sensitivity function $1/K_n$

Modelling,
Calibration,
Approximation errors

Comparable quantity

X

Ordinary least-squares

$\tilde{X}$

Inversion of W matrix

Example: 2D Integrated Field Reconstruction by Rotating Coil Mapping

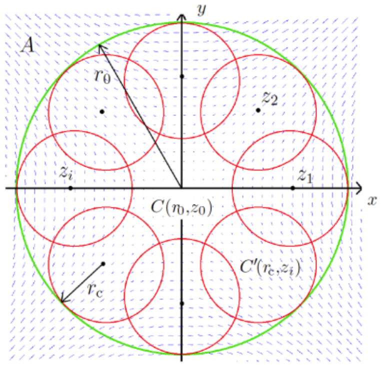

$$C'_n(z_i) = \sum_{k=n}^{\infty} C_k(z_0) \binom{k-1}{k-n} \left(\frac{z_i}{r_0}\right)^{k-n}$$

$$C_n(r_c) = \left(\frac{r_c}{r_0}\right)^{n-1} C_n(r_0)$$

$$w_{n,k}^{(i)} = \binom{k-1}{k-n} \left(\frac{z_i}{r_0}\right)^{k-n} \left(\frac{r_c}{r_0}\right)^{n-1}$$

$$[W_i] = \begin{pmatrix} w_{1,1}^{(i)} & \cdot & \cdot & \cdot & \cdot & \cdots & w_{1,K}^{(i)} \\ 0 & \cdot & \cdot & \cdot & \cdot & \cdot & \cdots \\ 0 & 0 & \cdot & \cdot & w_{n,k}^{(i)} & \cdot & \cdots \\ \vdots & \vdots & \ddots & \cdot & \cdot & \cdots & \\ 0 & 0 & \cdots & 0 & \cdot & w_{N-1,K-1}^{(i)} & w_{N-1,K}^{(i)} \end{pmatrix}$$

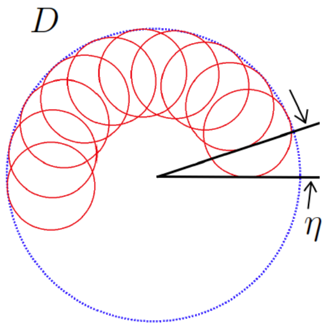

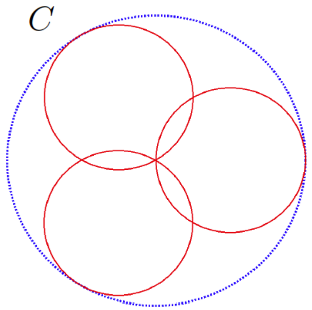

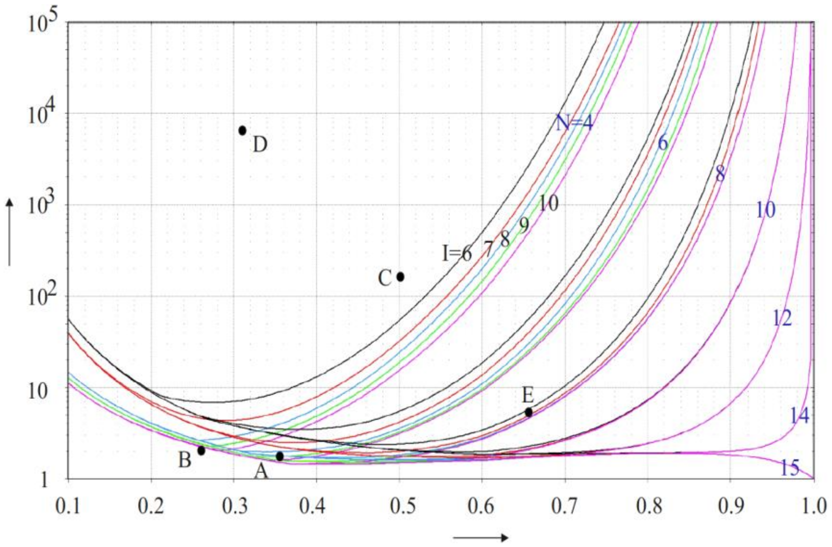

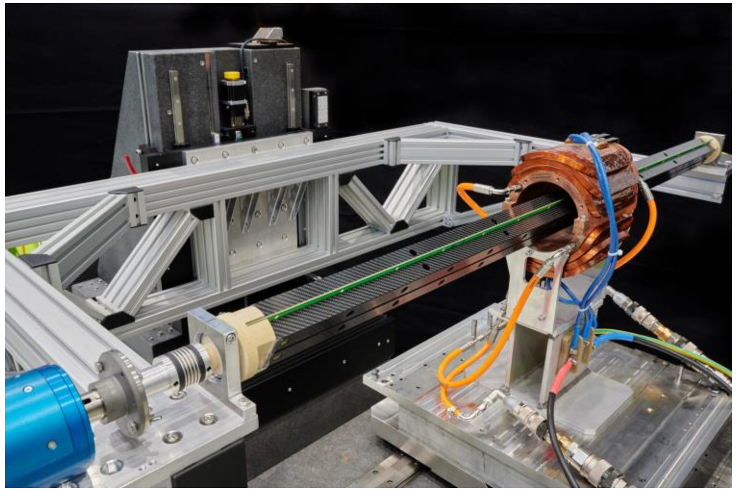

Example: 2D Integrated Field Reconstruction by Single Stretched Wire

Physical object (magnet)

Magnetic flux density in the magnet bore

Capture noise

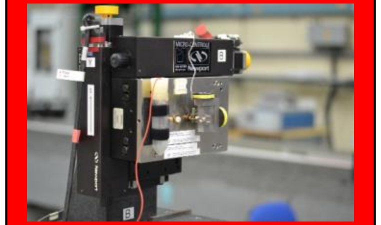

Read-out noise

Raw signal (voltages)

AD-conversion
Digital integration,
Drift correction

Fluxes

Magnetic flux density expressed as basis functions on a 2D boundary mesh

$$C\,A(\mathbf{r}) + \int_{\Gamma} -\partial_{\mathbf{n}_a} A\, u^*(\mathbf{r},\mathbf{r}')\,\mathrm{d}a' + \int_{\Gamma} A\,\partial_{\mathbf{n}_a} u^*\,\mathrm{d}a' = 0$$

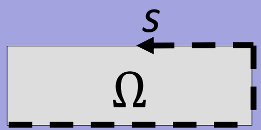

Numerical errors

Prediction

Observation function

Field Quality

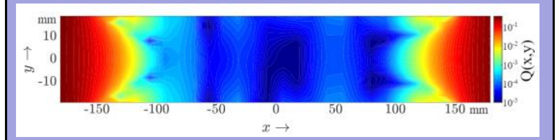

Magnetic flux through boundary

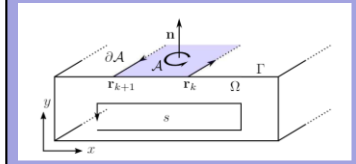

$$\Phi_{\mathcal{A}} = \iint_{\mathcal{A}} \mathbf{B}\cdot\mathrm{da}$$

Quantity of interest

Comparable quantity

Modelling,
Calibration,
Approximation errors

X

Weighted least-squares

$\tilde{X}$

2D Field inversion

Example: 2D Integrated Field Reconstruction by Single Stretched Wire

$$C\,A(\mathbf{r}) + \int_\Gamma -\partial_{\mathbf{n}_a} A\, u^*(\mathbf{r},\mathbf{r}')\,\mathrm{d}a' + \int_\Gamma A\,\partial_{\mathbf{n}_a} u^*\;\mathrm{d}a' = 0$$

	$u^*(\mathbf{r},\mathbf{r}')$	$q^*(\mathbf{r},\mathbf{r}') := \partial_{\mathbf{n}_a} u^*$	C
2D	$-\frac{1}{2\pi}\ln\lvert\mathbf{r}-\mathbf{r}'\rvert$	$-\frac{(\mathbf{r}-\mathbf{r}')\cdot\mathbf{n}_a}{2\pi\lvert\mathbf{r}-\mathbf{r}'\rvert^2}$	$\frac{\beta}{2}$
3D	$\frac{1}{4\pi\lvert\mathbf{r}-\mathbf{r}'\rvert}$	$-\frac{(\mathbf{r}-\mathbf{r}')\cdot\mathbf{n}_a}{4\pi\lvert\mathbf{r}-\mathbf{r}'\rvert^3}$	$\frac{\Theta}{4\pi}$

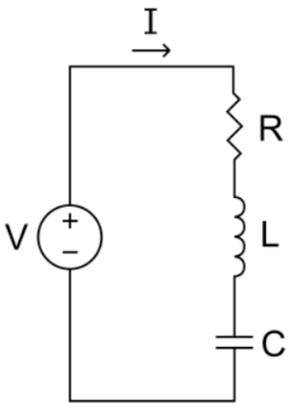

$$RI(t) + L\frac{dI(t)}{dt} + V(0) + \frac{1}{C}\int_0^t I(\tau)\,d\tau = V(t)$$

$$\frac{d^2}{dt^2}I(t) + \frac{R}{L}\frac{d}{dt}I(t) + \frac{1}{LC}I(t) = 0$$

$$\zeta = \frac{R}{2}\sqrt{\frac{C}{L}}$$

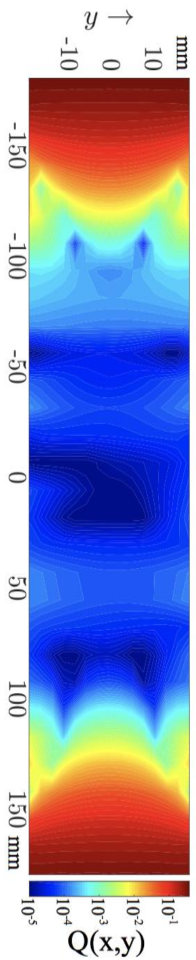

Reconstructed from Boundary Data

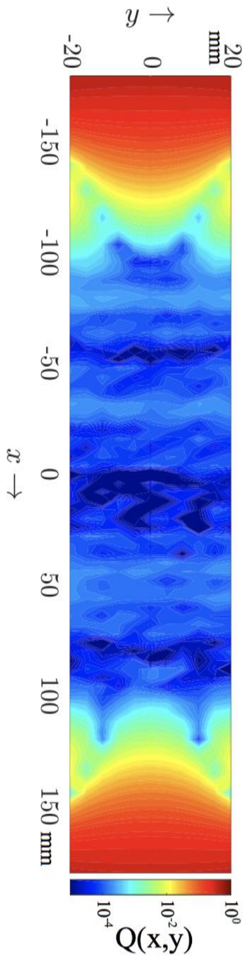

Grid map

Example: 3D Multipole Fields in Magnet Ends

Magnetic flux density parameterized by pseudo-multipoles at the surface of cylinder

$$B_n(r_0,z) = -\mu_0 r_0^{n-1}\overline{C}_n(r_0,z) =$$
$$-\mu_0 r_0^{n-1}\left(n\,C_{n,n}(z) - \frac{(n+2)C_{n,n}^{(2)}(z)}{4(n+1)}r_0^2 + \frac{(n+4)C_{n,n}^{(4)}(z)}{32(n+1)(n+2)}r_0^4 - \dots\right)$$

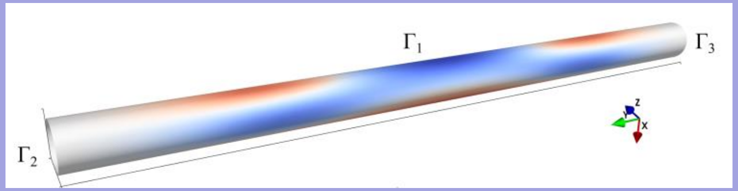

Numerical errors

Prediction

Observation function

Magnetic vector potential for particle tracking

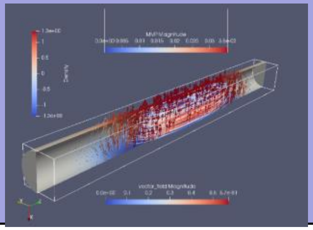

Flux linked with the coil area

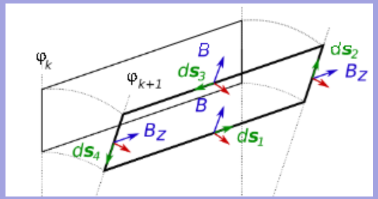

Quantity of interest

Comparable quantity

Modelling,
Calibration,
Approximation errors

Physical object (magnet)

Magnetic flux density in the magnet bore

Capture noise

Rotating coil

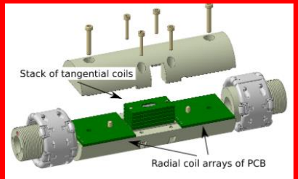

Read-out noise

Raw signal (voltages)

AD-conversion
Digital integration,
Drift correction

Flux increments

X

Weighted least squares

$\tilde{X}$

3D Field inversion

Example: 3D magnetic field in curved magnets

$$\boldsymbol{\alpha} = \mathbf{n} \times (\mathbf{H}_1 - \mathbf{H}_2) = \mathbf{n} \times [\![\mathbf{H}]\!]_{12}$$

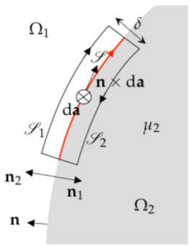

Physical object (magnet)

Magnetic flux density in the magnet bore

Capture noise

Read-out noise

Raw signal
(Hall voltages)

Magnetic flux density parameterized by stream function on 3D domain boundary

$$\boldsymbol{\alpha}(\mathbf{r}') := \frac{1}{\mu}\partial_{\mathbf{n}_a} A(\mathbf{r}')$$

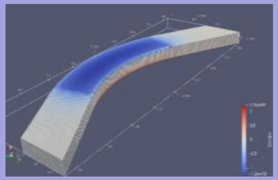

Numerical errors

Prediction

Observation function

Magnetic vector potential for particle tracking

$$\frac{\mathrm{d}\boldsymbol{q}}{\mathrm{d}t} = \frac{\partial H}{\partial \boldsymbol{p}}, \qquad \frac{\mathrm{d}\boldsymbol{p}}{\mathrm{d}t} = \frac{\partial H}{\partial \boldsymbol{q}}$$

$$H = c\sqrt{(\boldsymbol{p} - q\boldsymbol{A})^2 + m^2c^2} + q\phi.$$

Voltage response of the Hall probe

$$U(B) = \sum_{k=1}^{K} c_k\,|\boldsymbol{B}|^k\, Y_k^l(\theta,\varphi)$$

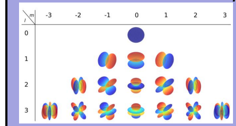

Quantity of interest

Comparable quantity

Modelling,
Calibration,
Approximation errors

X

Maximum a posteriori

$\tilde{X}$

3D Field inversion

Example: Generalized Field Description of Dipole

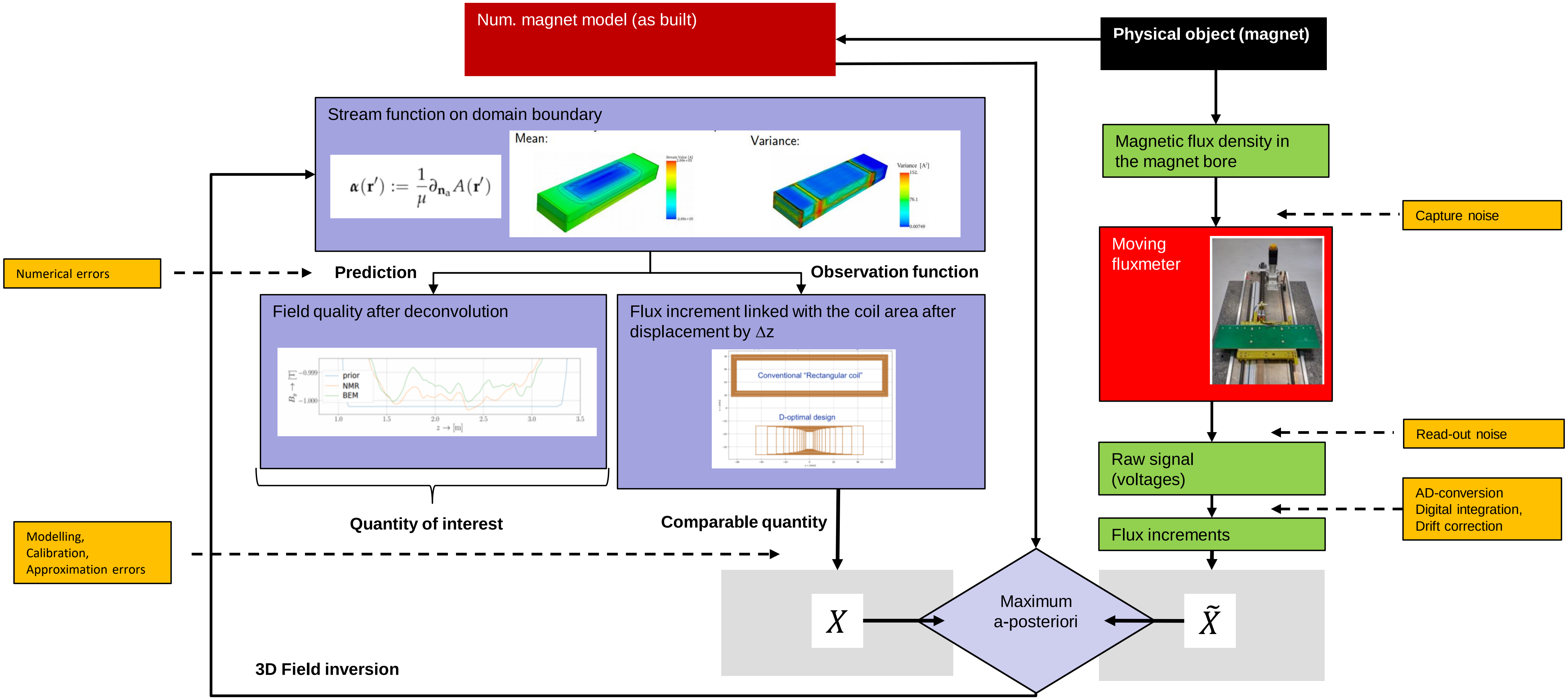

Avatar (Generalized Field description of dipole field)

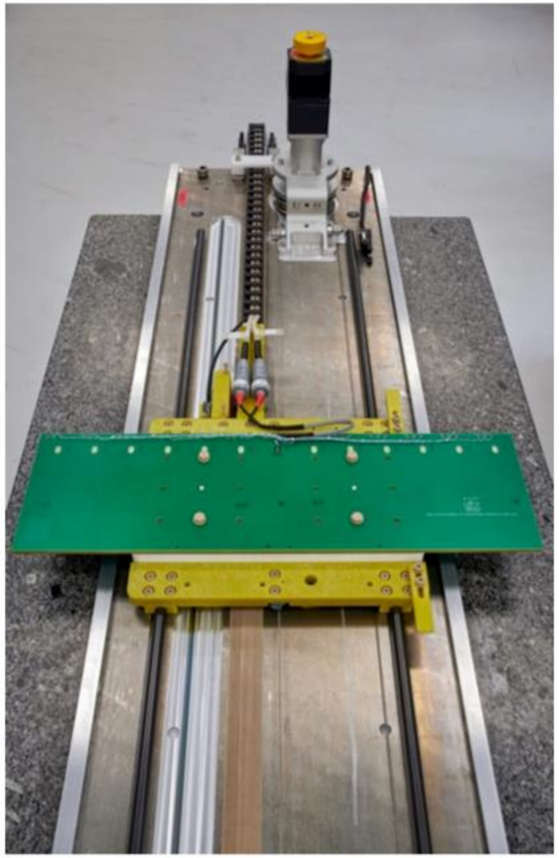

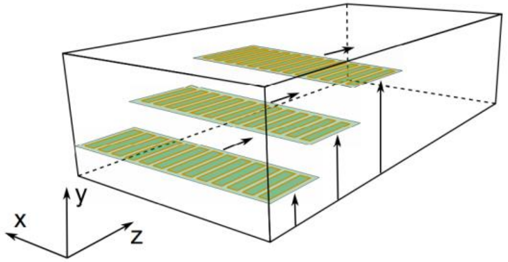

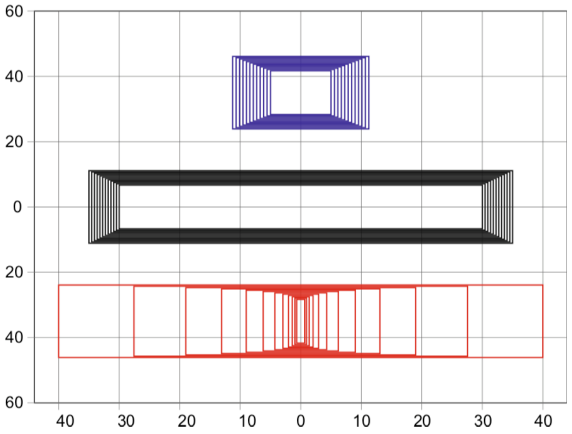

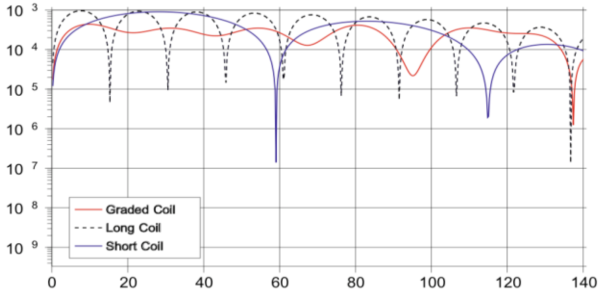

Mean:

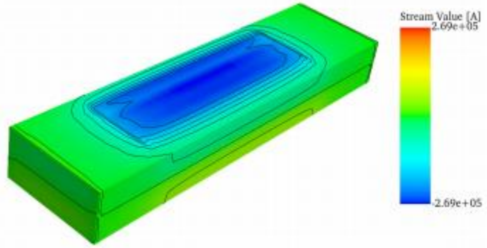

Variance:

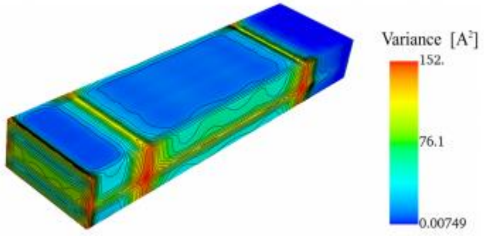

- Comparing field reconstruction with NMR in the homogeneous region

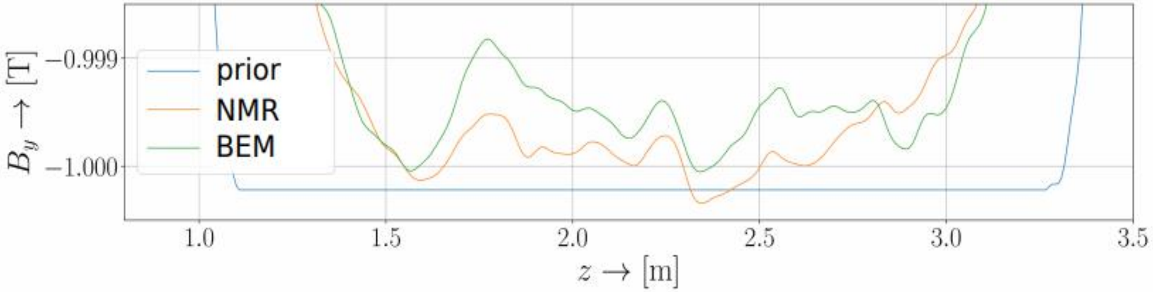

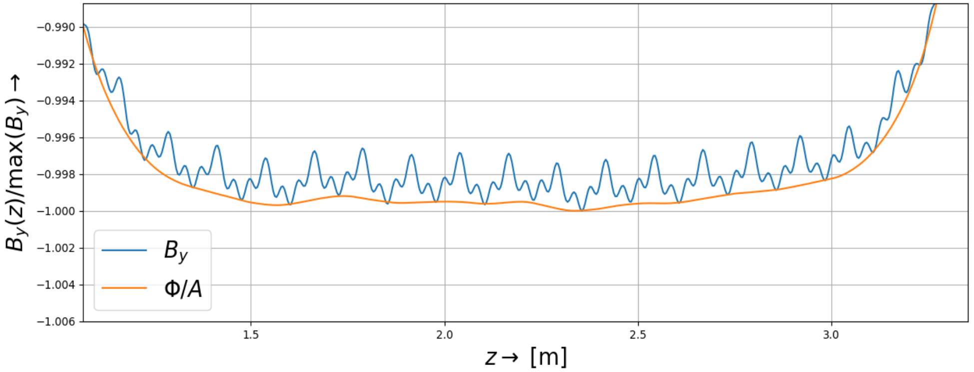

The Avatar and Twin (tracing of manufacturing tolerances and errors)

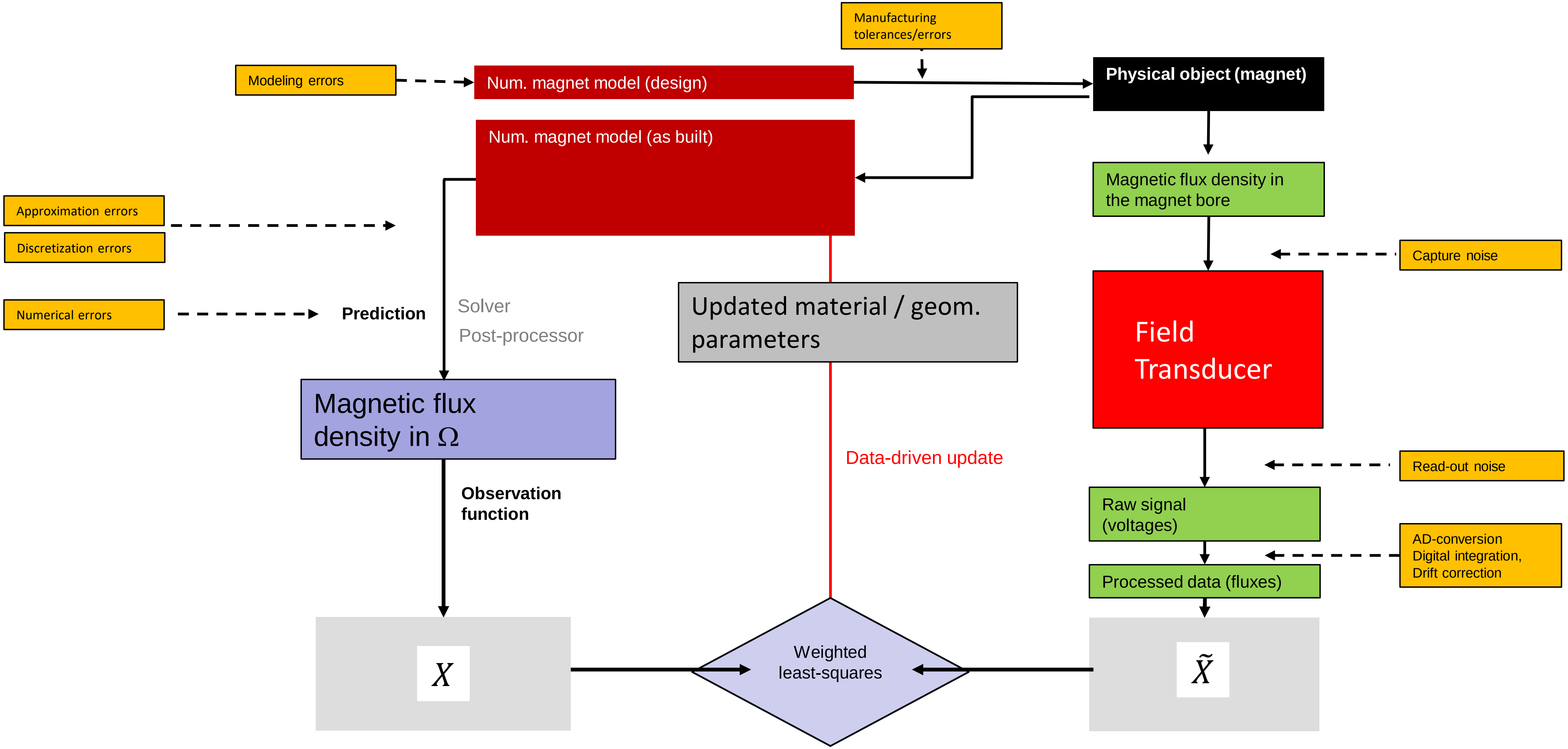

Example: Iron Magnetization

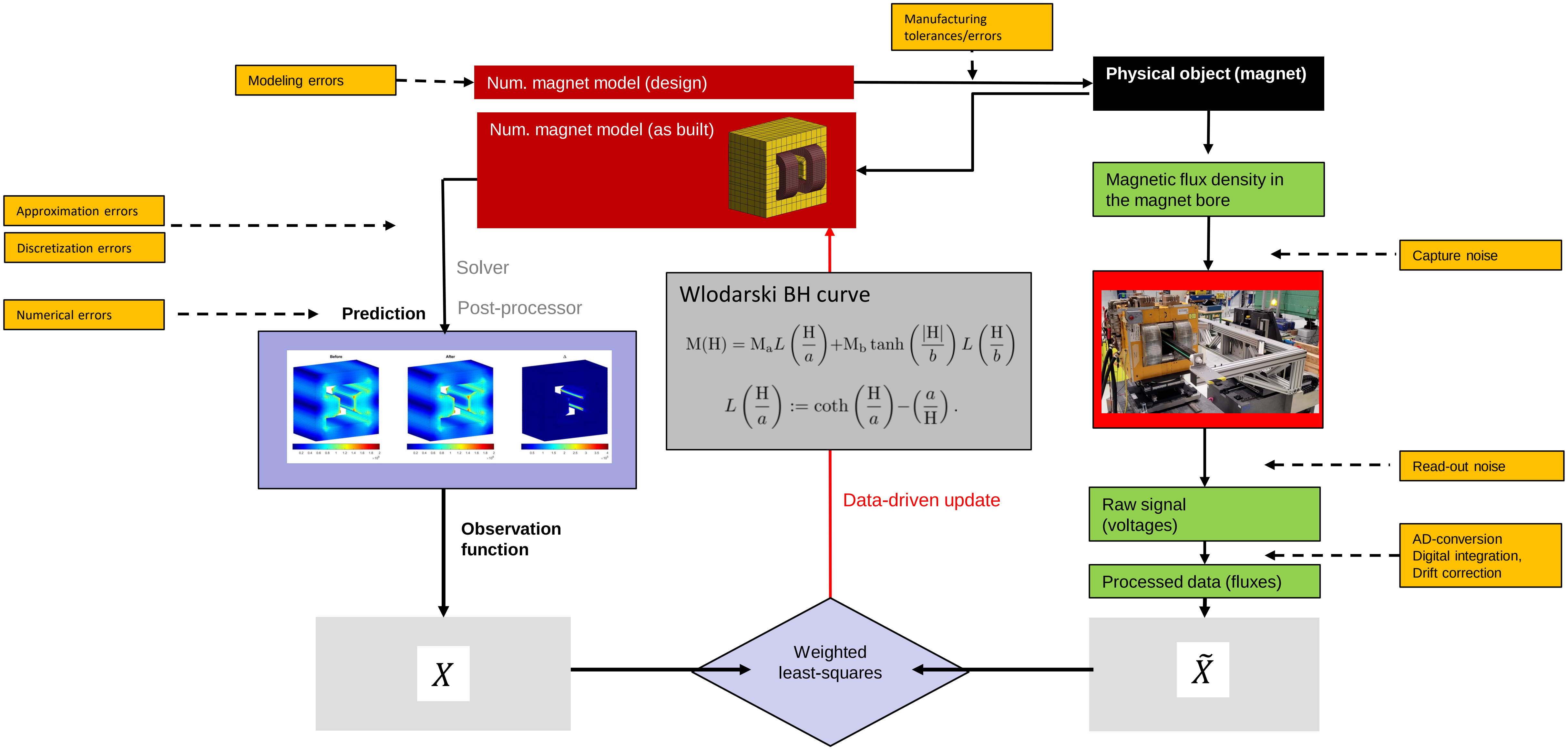

Example: Iron Magnetization

$$\mathrm{M}(\mathrm{H}) = \mathrm{M_a} L\left(\frac{\mathrm{H}}{a}\right) + \mathrm{M_b} \tanh\left(\frac{|\mathrm{H}|}{b}\right) L\left(\frac{\mathrm{H}}{b}\right) \quad \text{where} \quad L\left(\frac{\mathrm{H}}{a}\right) := \coth\left(\frac{\mathrm{H}}{a}\right) - \left(\frac{a}{\mathrm{H}}\right).$$

A/m	Initial values	Range	Final values
M_a	1.347×10^6	$\pm 25\%$	1.588×10^6
a	452.2	$\pm 50\%$	623.6
M_b	0.3197×10^6	$\pm 50\%$	0.252×10^6
b	8090	$\pm 50\%$	9175

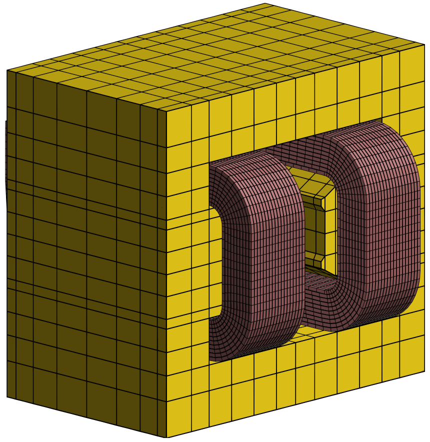

Magnetization Updating

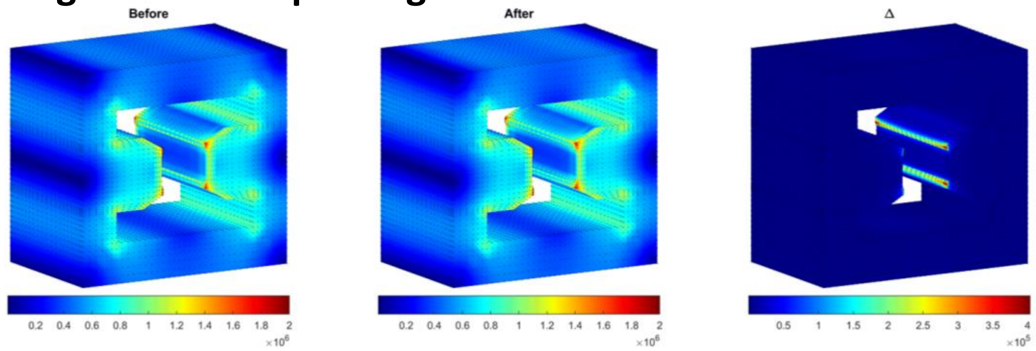

To do: Geometry versus B/H identified by **local** and **integral** measurements

Model	Magnet
• 36000 bricks of 24 dofs. • 992 elem., 10600 dofs.	• Aperture 148 mm, length 400 mm. • Maximum current 240 A. • Yoke: AISI 1010 steel, solid blocks.

Example: Persistent Currents in Orbit Corrector

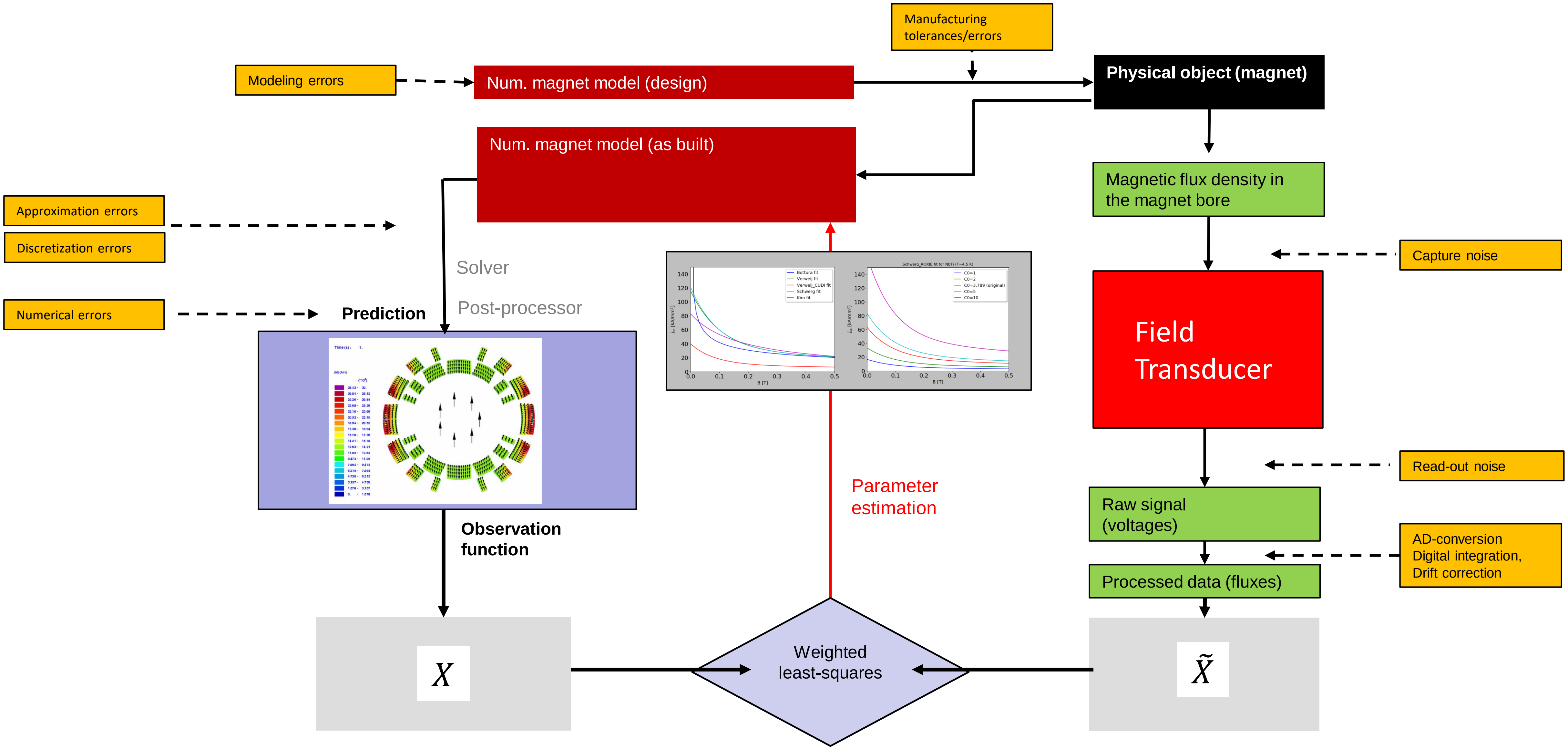

Example: Persistent Currents in Orbit Corrector

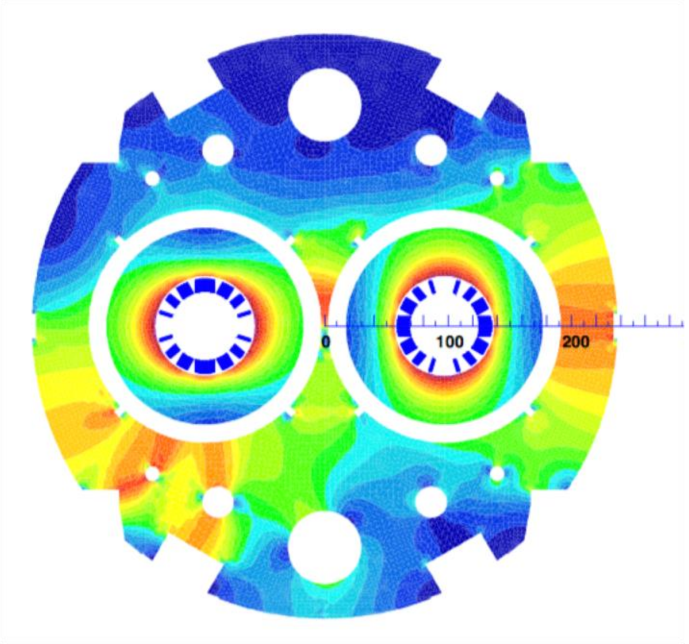

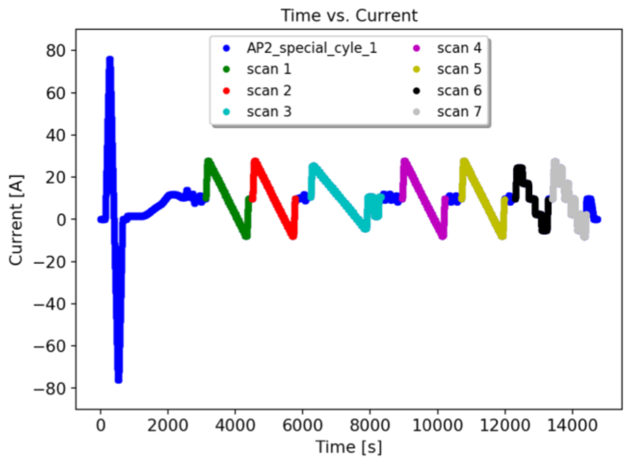

Special test cycles

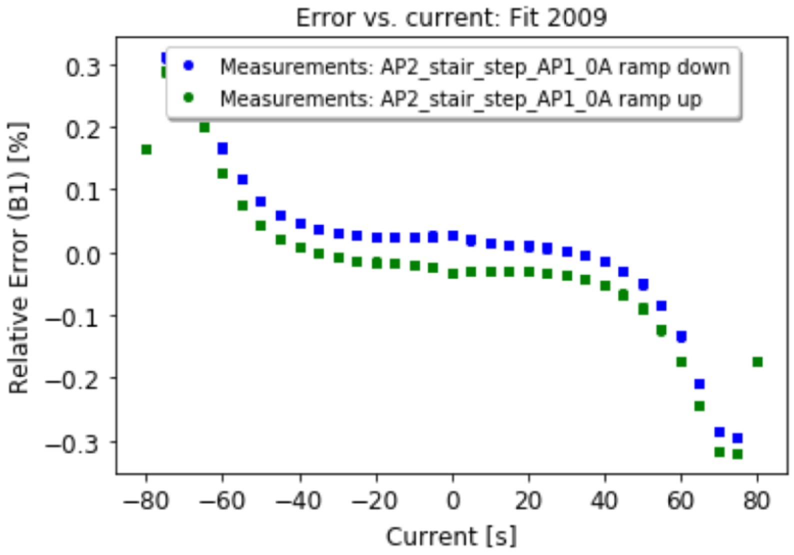

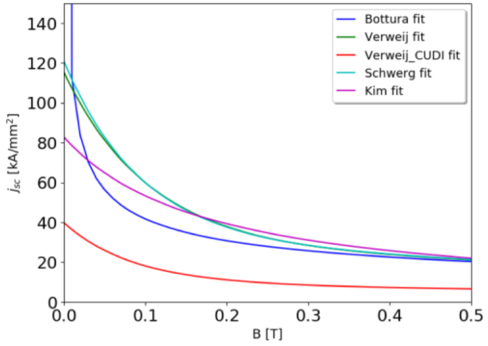

Fit functions

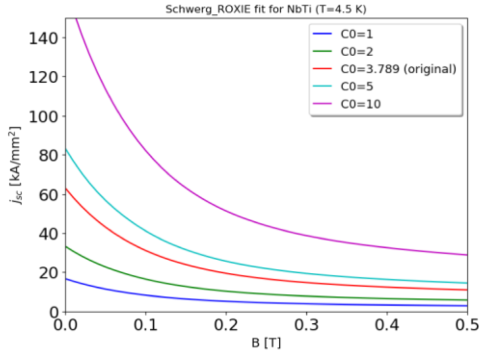

Parameters

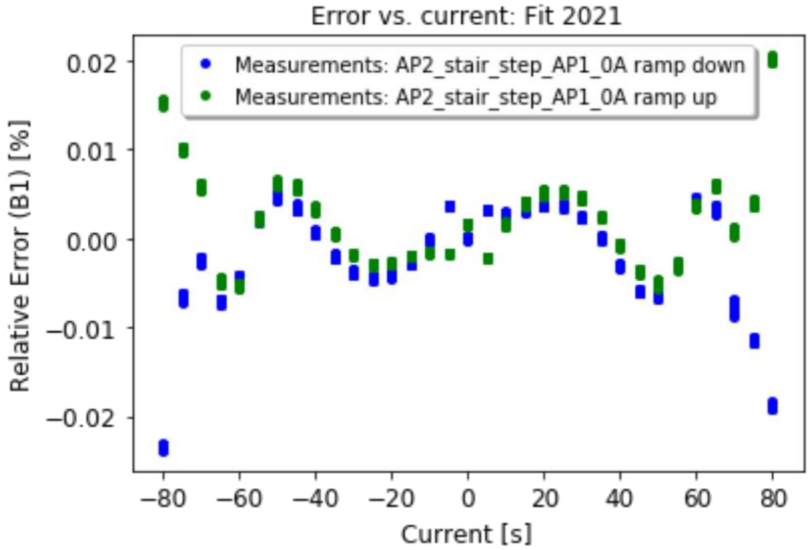

The Avatar and Twin (generalized field description with updated modes)

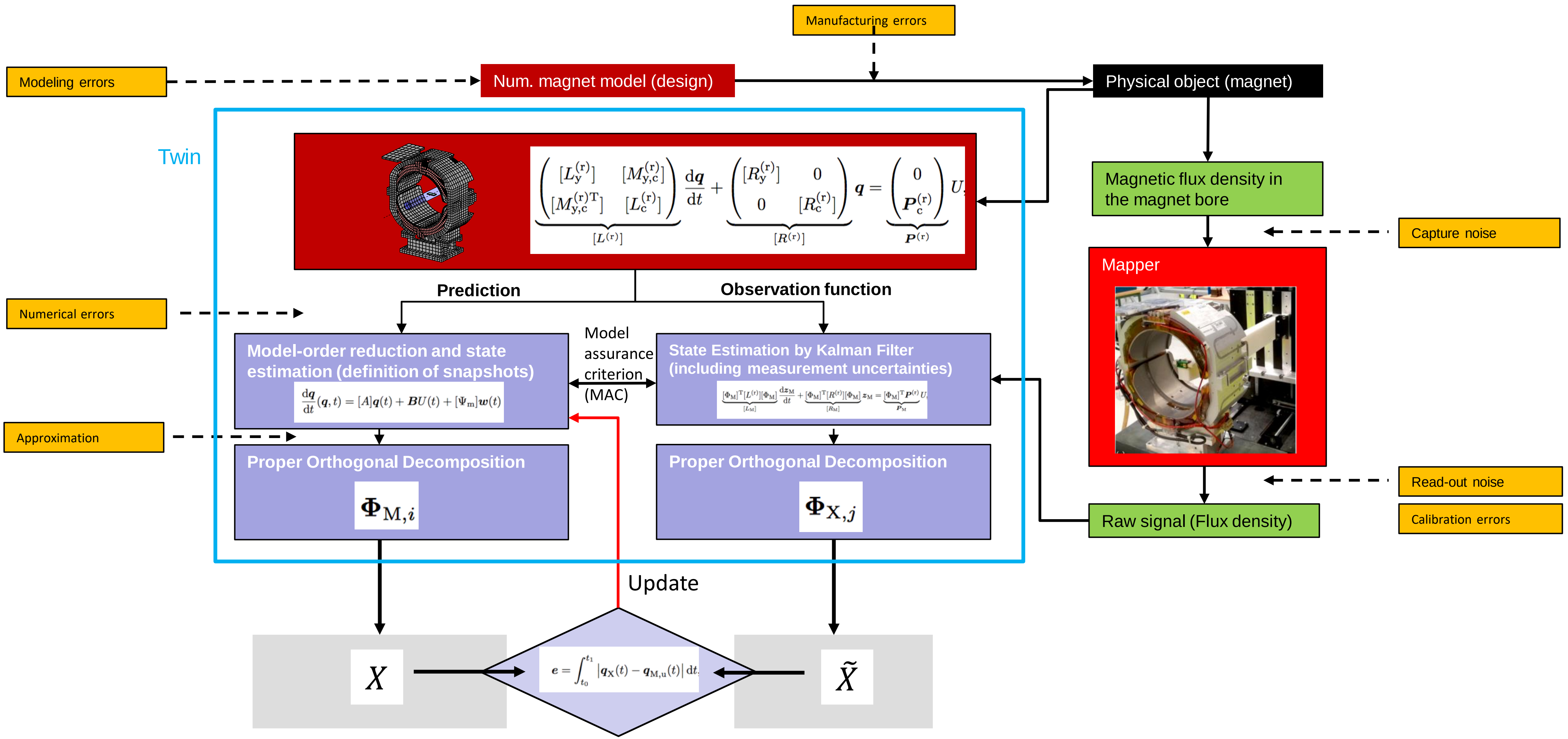

Example: Eddy-Current Induced Field Errors

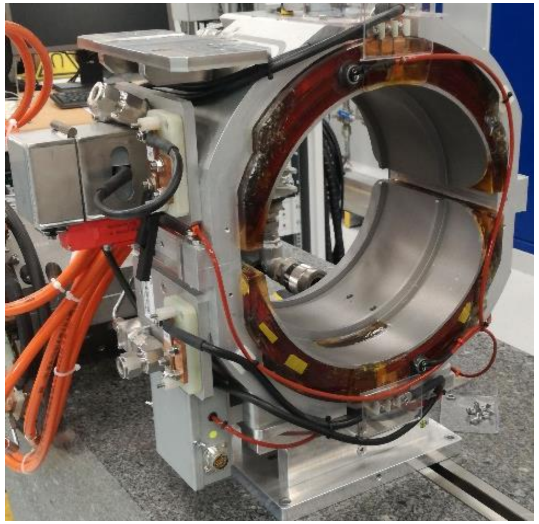

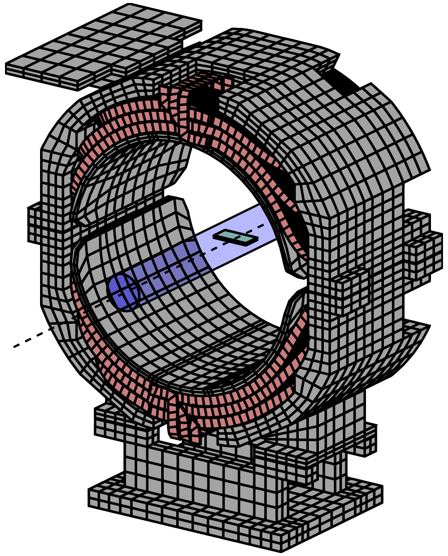

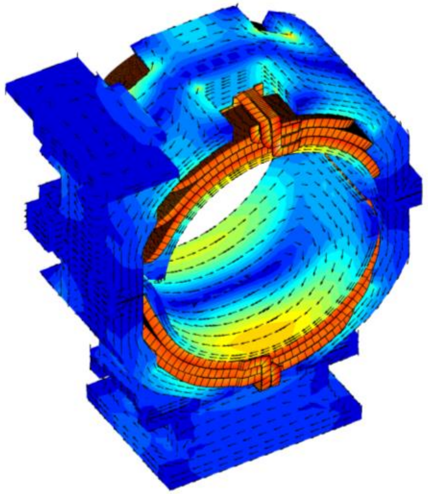

Simulated

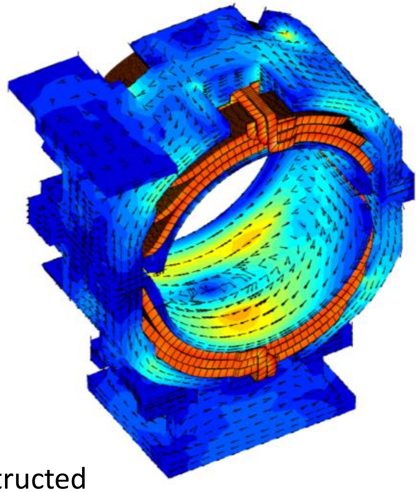

Reconstructed

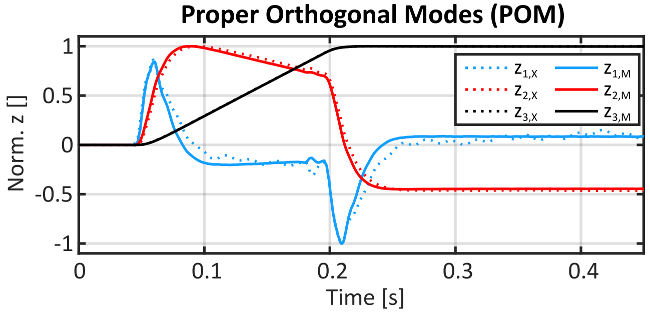

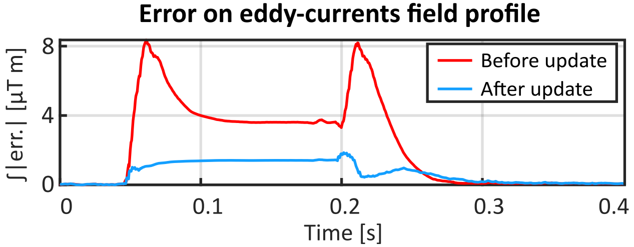

Magnet	Model
• Bore diameter 136 mm. • Good Field Region 40 mm. • Maximum current 45 A. • Maximum rate 400 As^{-1}.	• 19000 bricks of 18 dofs (800 modes preserved) • 5800 elem., 88000 dofs (2800 modes preserved)

Next Steps

- ➔ Metric for expressing the accuracy measured and calculated field distributions
- ➔ Regularization methods for the inverse problem: model based or statistical prior
- ➔ Identification of physical, empirical, and neural-network models for
  - stress dependent superconductor magnetization,
  - iron hysteresis,
  - 3D eddy-currents,
  - passive correction circuits (e.g., pole-face windings in PS magnets).
- ➔ Proper orthogonalization applied to nonlinear field problems
- ➔ Convergence studies for the twin of the eddy current induced field error in the air-coil magnet
- ➔ Global (wire) versus local (scanner) measurements for parameter identification in normal conducting magnet
- ➔ Concept for model-driven systems engineering
  - database management structures,
  - software for magnetic measurements,
  - quality assurance for magnet production